DOI: 10.1590/2317-4889201820170061

ARTICLE

Sedimentary provenance in the southern sector of the São Francisco Basin, SE Brazil

Gustavo Macedo de Paula-Santos[1]*, Marly Babinski[1]

ABSTRACT: *We present new Sm-Nd, U-Pb and Hf isotope geochronological data for the siliciclastic rocks in the southern sector of the São Francisco Basin. An abrupt change in the Sm-Nd data is observed from the Carrancas Formation's oligomitic conglomerates (T_{DM} ages between 2.7 and 3.3 Ga; $\varepsilon_{Nd(550\ Ma)}$ values between -25.09 and -17.98), its finer facies, and the finer facies of the the Moema Laminite (T_{DM} ages from 1.4 to 2.1 Ga; $\varepsilon_{Nd(550\ Ma)}$ values between -9.46 and -5.59). No further significant changes in the Sm-Nd data occur farther upwards in the Bambuí Group (Sm-Nd T_{DM} ages within the 1.3-2.0 Ga interval; $\varepsilon_{Nd(550\ Ma)}$ values from -9.53 to -4.09), showing a lack of reorganization in the source areas throughout the deposition of the basin. This is yet another argument to dismiss an unconformity within the Bambuí Group. The presence of the index fossil Cloudina sp. in the lower Sete Lagoas Formation makes the glaciation probably Late Ediacaran in age. U-Pb ages for detrital zircons of the Bambuí Group range from the Archean to the early Ediacaran, but the current data is insufficient to distinguish between the contribution from sources in the Brasília and Araçuaí belts.*

KEYWORDS: *Detrital zircon U-Pb dating; Sm-Nd isotopes provenance; Carrancas Formation; Moema Laminite; Bambuí Group.*

INTRODUCTION

The geological history of the São Francisco Basin (east-central Brazil; Fig. 1) is a puzzle and has many implications for the West Gondwana assembly at the Ediacaran-Cambrian boundary. A large data set shows that its sedimentary rocks were deposited in a foreland basin fixed over the homonymous craton as a response to the crustal load of the western Brasília Belt (Fig. 1). Intriguingly, the timing of the deposition of most of the sediments is constrained to be younger than 560 Ma (Warren *et al.* 2014, Paula-Santos *et al.* 2015), which is much younger than the orogen's metamorphic peak (~630 Ma; Pimentel *et al.* 1999, Pimentel 2016). As such, this represents early stages of subsidence in the basin. Although the Brasília Belt has a wide range of magmatic rocks spanning through the Ediacaran, the plutonism dated at ca. 540 Ma is considered anorogenic (Pimentel 2016), meaning that refinements in the timing regarding the subsidence and filling of the São Francisco Basin still need to be done. Also, by ca. 550 Ma the Araçuaí orogen was already built at the eastern margin of the craton (Fig. 1; Pedrosa-Soares *et al.* 2011), but its contribution to the basin filling is not fully understood. Seismic sections show that the belt mainly deforms the sediments and there is hardly any sedimentation wedge over the craton (Zalán & Romeiro-Silva, 2007). Exposed rocks that could potentially be sources of sediments dated at ca. 560 Ma are described in the Southern Brasília Orogen (Coelho *et al.* 2017) and the Ribeira Belt (Heilbron *et al.* 2008) and they go to the south of the São Francisco craton, so that they may also have contributed to the basin filling.

Furthermore, researchers have not achieved an agreement about the age of the glaciation recorded at the base of the Bambuí Group, the main geological unit of the São Francisco Basin. This unit is comprised of carbonate-siliciclastic rocks that overlie the basal glaciogenic deposits of the Jequitaí Formation and its correlatives in the cratonic and marginal belts areas. The basal unit of the Bambuí Group is the Sete Lagoas Formation (Fig. 2), which is mostly composed of carbonate rocks with very negative $\delta^{13}C$ values at the base (Alvarenga *et al.* 2007, 2014, Vieira *et al.* 2007, Caxito *et al.* 2012, Kuchenbecker *et al.* 2016, Paula-Santos *et al.* 2017). This geological record is in agreement with the Snowball hypothesis (Hoffman *et al.* 1998, Hoffman & Schrag 2002) that postulates at least three periods of extreme climatic shifts during the Cryogenian and Ediacaran

[1]Instituto de Geociências, Universidade de São Paulo – São Paulo (SP), Brazil. *E-mails: gustavomps@yahoo.com.br, babinski@usp.br*

*Corresponding author.

Manuscript ID: 20170061. **Received on:** 04/28/2017. **Approved on:** 01/22/2018.

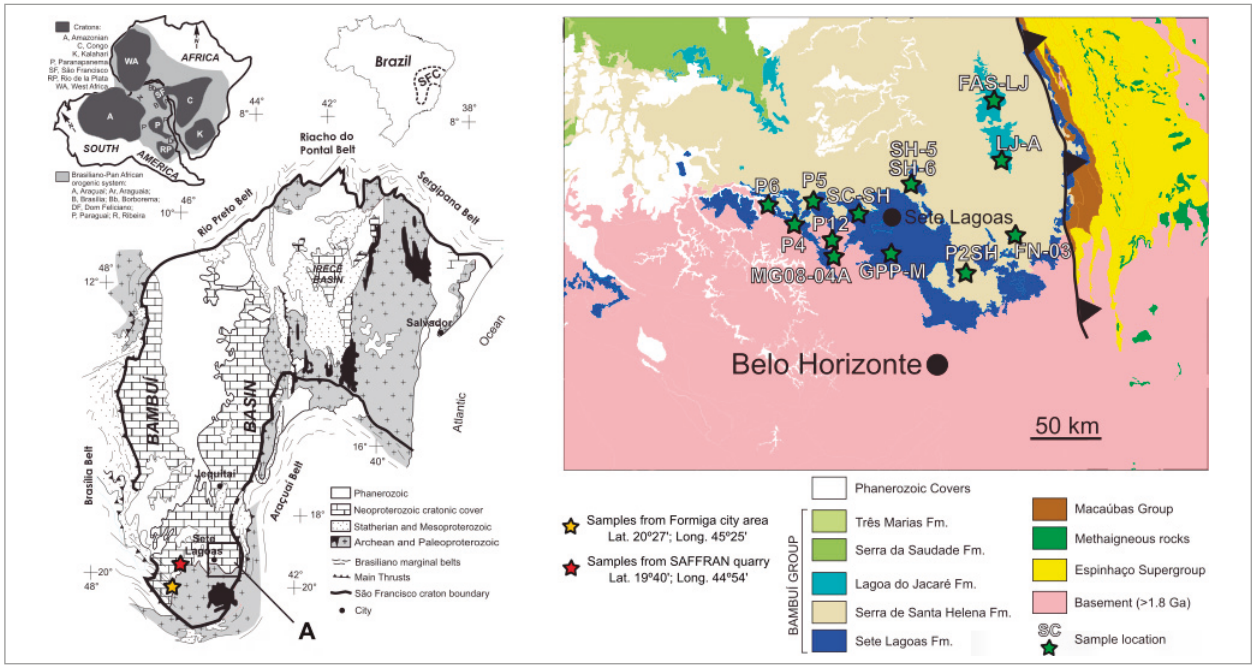

Figure 1. A geological sketch of West Gondwana at ca. 540 Ma, a map of the São Francisco Craton (modified from Alkmim *et al.* 2006) and location of the samples studied in this work. Samples from the Formiga city area include the Moema Laminite rocks (MG03 27A, MG02-11 and 13, MG03-21, 22 and 23A, MG04-42 and 43; Tab. 1), siltites from the Sete Lagoas Formation (samples MG05-06, 09, 10, 12 and 13; Tab. 1), and siltites from the Serra de Santa Helena Formation (samples MG03-24 and 25, and MG05-11; Tab. 1). Samples from the SAFFRAN quarry are the Moema Laminite siltites (samples MG02-14b, and MG04-41A). In the detailed map, samples MG08-08 and P12 belong to the Carrancas Formation, samples P4, P5, P6, FN-03 and GPP-M are from the Sete Lagoas Formation, samples P2SH, SH-05, SH-06 and SC-SH are from the Serra de Santa Helena Formation, and samples FAS-LJ and LJ-A belong to the Lagoa do Jacaré Formation.

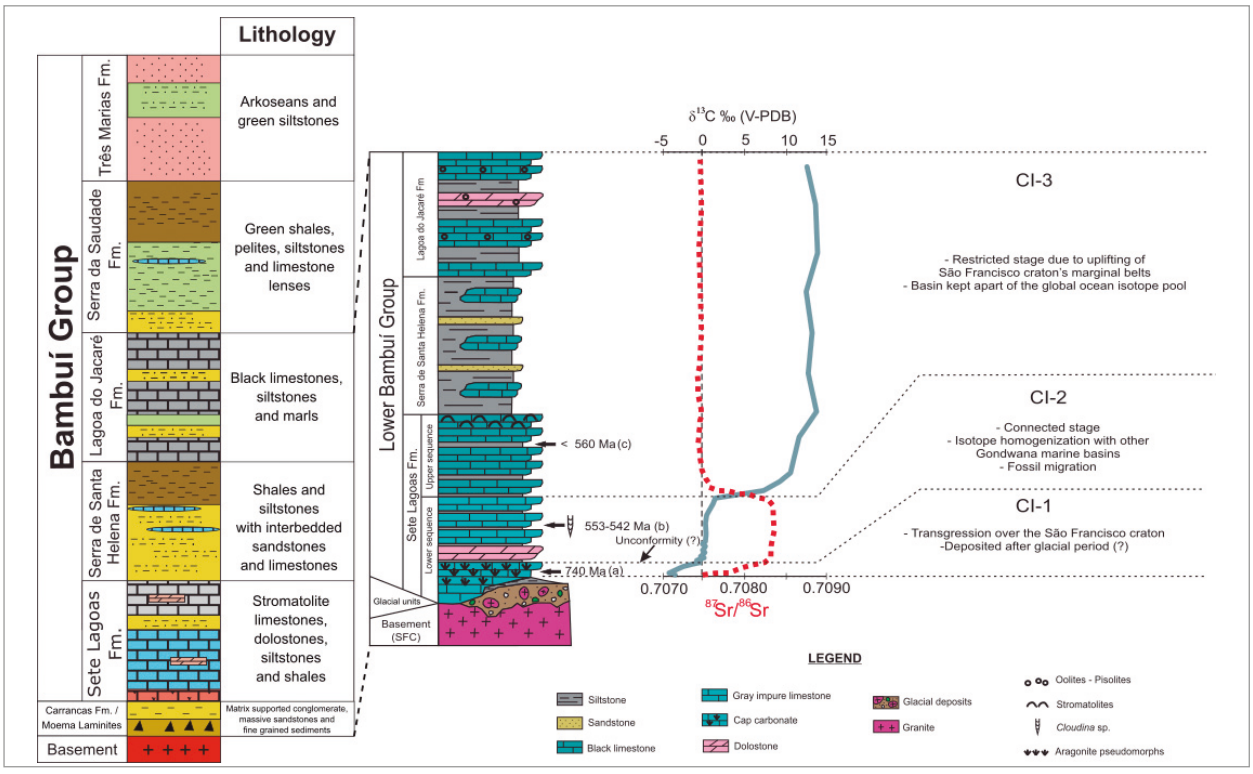

Figure 2. The stratigraphic column of the Bambuí Group (after Dardenne 1978) and its subdivision into Chemostratigraphic Intervals (CI — Paula-Santos *et al.* 2017). The ages shown were extracted from: (a) Babinski *et al.* (2007); (b) Warren *et al.* (2014); (c) Paula-Santos *et al.* (2015).

(Halverson *et al.* 2005). These are named Sturtian (~720 Ma), Marinoan (~635 Ma) and Gaskiers (~582 Ma).

Babinski *et al.* (2007) dated the cap carbonates of the Sete Lagoas Formation at 740 ± 22 Ma (Pb-Pb isochron age) and correlated the glaciation of the São Francisco Basin to the Sturtian period. On the other hand, Caxito *et al.* (2012) and Alvarenga *et al.* (2014) proposed a Marinoan age for the glaciation, based on isotope chemostratigraphy on the overlying carbonate rocks. However, the presence of the index fossil *Cloudina* sp. at the middle portion of the Sete Lagoas Formation (Warren *et al.* 2014) has an important implication for the propositions of these Cryogenian ages. Either an unconformity yet to be found separates the cap carbonates from the rest of the Bambuí Group, or the lowermost part of the Sete Lagoas Formation records the entire Ediacaran period. Based on a stratigraphic and chemostratigraphic analysis, Kuchenbecker *et al.* (2016) concluded that the existence of an unconformity is unlikely, and proposed that the basal diamictites may be Late Ediacaran in age.

Within this debate we present new Sm-Nd data for the siliciclastic rocks of the Bambuí Group and its basal diamictites. Additionally, U-Pb SHRIMP ages and Hf isotope data of detrital zircon grains retrieved from a sandstone sample of the Serra de Santa Helena Formation (Fig. 2) are also presented. This work is an effort to track the sedimentary sources of the São Francisco Basin and its relationship with the surrounding orogens, as well as to shed light on the age of the diamictites.

GEOLOGICAL SETTING

The São Francisco Basin is comprised of Neoproterozoic-Cambrian sedimentary rocks that cover more than 300,000 km^2 of the homonymous craton in east-central Brazil (Fig. 1). There are exposures of the basement (> 1.8 Ga), which occur in the southern and north-eastern areas of the craton (Teixeira *et al.* 2000, Alkmim & Martins-Neto 2012).

The base of the sedimentary cover is composed of sparse glacial units of the Jequitaí Formation, interpreted as of continental (Rocha-Campos & Hasui 1981, Karfunkel & Hoppe 1988, Martins-Neto & Hercos 2002) or glaciomarine origin (Rocha Campos *et al.* 1996, Cukrov *et al.* 2005, Chaves *et al.* 2010, Uhlein *et al.* 2011). In spite of several tectonic discontinuities, the glacial unit has correlating units in the marginal belts: the glacial formations of the Macaúbas Group in the Araçuaí Belt and the Cubatão Formation of the Ibiá Group in the Brasília Belt (Uhlein *et al.* 1999, Dardenne 2000, Martins-Neto *et al.* 2001, Pedrosa-Soares *et al.* 2011, Babinski *et al.* 2012). In the cratonic area, the Carrancas Formation (Dardenne 1978, Vieira *et al.* 2007, Uhlein *et al.* 2012) and the Moema laminites (Rocha-Campos *et al.* 2011) are at the base of the Bambuí Group in the southern sector of the São Francisco Basin, although the glacial origin of the first unit is debatable (Caxito *et al.* 2012, Uhlein *et al.* 2016).

The Bambuí Group is the main unit of the São Francisco Basin and is composed of carbonate-siliciclastic rocks that either overlie the glacial unit or are in sharp contact atop the basement (Dardenne 1978). It records a marine transgression in a foreland basin set over the craton in response to the Brasília and Araçuaí belts crustal overload. The unit crops out throughout the craton and the western Brasília Belt, but not in the eastern orogen (Martins-Neto *et al.* 2001, Zalán & Romeiro-Silva 2007, Alkmim & Martins-Neto 2012, Reis & Suss 2016). Shear zones with well-developed foliation and stretching lineation separate the basement and sedimentary cover, and the metamorphism in the studied area is low graded.

Dardenne (1978) subdivided the Bambuí Group into five units (Fig. 2), from base to top:

- the Sete Lagoas Formation that is composed of limestones and dolostones with interbedded marls and siltites (thickness ≤ 500 m);
- the Serra de Santa Helena Formation, which is comprised of mainly siltstones with interbedded shales, sandstones and limestones (640 m);
- the Lagoa do Jacaré Formation that consists of oolithic limestones, siltstones and marlstones (350 m);
- the Serra da Saudade Formation, which displays siltstones, green shale and minor occurrences of limestones (100 m);
- the Três Marias Formation, which is constituted of arkosic sandstones and siltstones (100 m).

The thicknesses here shown were extracted from Iglesias and Uhlein (2009).

The age of the rocks of the São Francisco Basin remains controversial. The basal carbonate rocks of the Sete Lagoas Formation display very negative $\delta^{13}C$ values, which are similar to other Neoproterozoic cap carbonates (Alvarenga *et al.* 2007, 2014, Vieira *et al.* 2007, Caxito *et al.* 2012, Kuchenbecker *et al.* 2016). Babinski *et al.* (2007) obtained a Pb-Pb isochron age of 740 ± 22 Ma in these carbonates, and correlated the glaciation to the Sturtian global event. Other researchers did not agree with this dating estimate and claimed that it was a Marinoan age (~635 Ma), based mainly on the presence of a thin basal pink dolostone, which is recognized worldwide as the start of the Ediacaran (Shields 2005), in addition to the presence of a negative carbon excursion found in these carbonates and in Sr isotope chemostratigraphy (Caxito *et al.* 2012, Alvarenga *et al.* 2014). But the recent findings of *Cloudina* sp. (Warren *et al.* 2014) and detrital zircons with

U-Pb around 560 Ma (Paula-Santos *et al*. 2015; Fig. 2) in the Sete Lagoas Formation, show that most of the Bambuí Group is Late Ediacaran / Early Cambrian in age. Unless a major unconformity between the cap carbonates and the rest of the deposits of the São Francisco Basin is assumed, the glaciogenic units are also likely to be Late Ediacaran in age (Kuchenbecker *et al*. 2016). Although some authors point to a sedimentation hiatus at such a stratigraphic position, because of seismic, sedimentary and isotopic features (Martins & Lemos 2007, Zalán & Romeiro-Silva 2007), studies on complete borehole (Kuchenbecker *et al*. 2016) and field (Perrella Jr. *et al*. 2017) sections refute that it represents a major regional unconformity. Therefore, a significant time gap at the base of the Sete Lagoas Formation is yet to be described.

Description of the samples

Two conglomerate samples from the Carrancas Formation (Tab. 1) were collected (Fig. 2). The outcrops consist of a monomitic to oligomitic matrix-supported conglomerate, deposited in basement valleys. The clasts are sub-angular to sub-rounded, with sizes ranging between 2 and 20 cm (largest side). They are dominantly composed of igneous rocks from the valley walls and have subordinated quartz vein fragments (Fig. 3A). The matrix has a greenish colour and is comprised of quartz and feldspar silt/sand with minor occurrences of carbonate cement. The size of the clasts decreases upwards and the conglomerate grades to orange / pink siltites with planar lamination (Fig. 3B). One siltite sample was collected.

Nine samples of the Moema Laminites were collected from two different localities. At the SAFFRAN quarry (Fig. 2), mudstone (sample MG04-41A) and varvite facies (MG02-14B) of the glacial succession were sampled. Striations in the bedding plane suggest that the sea ice touched the bottom of the basin during deposition (Rocha-Campos *et al*. 2011). The remaining samples were collected between Formiga and Bom Despacho cities (Fig. 2), where a sole glacial advance is recorded in a deformed tillite, overlain by a post-glacial laminate (Rocha-Campos *et al*. 2011). Varvite (n = 2; Tab. 1), siltite (n = 3) and mudstone facies (n = 2) of the glacial succession were sampled.

Ten samples from the Sete Lagoas Formation were collected, covering the three Chemostratigraphic Intervals (CI) proposed by Paula-Santos *et al*. (2017). One marl sample (P6, Tab. 1) interbedded in the CI-1 cap carbonates was retrieved in the Sambra quarry (for detailed stratigraphy see Vieira *et al*. 2007). We also collected eight samples of siltites from centimetric (5 to 15 cm thick) siliciclastic layers interbedded in the impure carbonate rocks of the CI-2 (Fig 2, Tab. 1). Finally, one marlstone interbedded in the dark grey limestones of the CI-3 (GPP-M) was sampled (Fig. 3C).

Eight samples from the Serra de Santa Helena Formation collected in several locations in the south of the São Francisco Basin were used in this study (Fig. 2). Five of them are siltites, which are the dominant lithotype of the unit (Fig. 3D), and three are sandstones found in some locations.

Finally, two samples from the Lagoa do Jacaré Formation were collected. Sample LJ-A is a fine sandstone interbedded in oolitic dark grey limestones (Fig. 3E), whereas sample FAS-LJ is a siltite (Fig. 3F) described as being within tilted limestones with carbonate intraclasts.

ANALYTICAL PROCEDURES

Thirty-two samples were analysed for Sm-Nd isotopic compositions. Samples P12 from the Carrancas Formation, GPP-M from the Sete Lagoas Formation, P2SH from the Serra de Santa Helena Formation, and LJ-A and FAS-LJ from the Lagoa do Jacaré Formation yielded enough zircon grains for U-Pb dating and Hf isotope analyses. Other samples did not provide enough of these minerals for U-Pb provenance. All of the sample preparation steps and isotope analyses were carried out at the Geochronological Research Center (CPGeo) of the University of São Paulo.

For the Sm and Nd isotopic analyses, whole rock samples were powdered and dissolved with HF, HNO_3 and HCl. Purification of Sm and Nd was performed by standard ion exchange chromatography procedures using RE and LN Eichrom resins. Isotope data were obtained by Thermal Ionization Mass Spectrometry (TIMS) using a Triton mass spectrometer (Thermo Fischer, Germany). The measured $^{143}Nd/^{144}Nd$ ratios were normalized to 0.7129 (DePaolo 1981). The mean value of the $^{143}Nd/^{144}Nd$ of the reference material JNdi-1 measured in the laboratory was 0.512102 ± 0.000002 (1σ). The Sm-Nd model ages are reported based on the depleted mantle model (DePaolo 1981) and are considered mean crustal residence ages. The $f_{Sm/Nd}$ and $\varepsilon_{Nd(550\ Ma)}$ parameters were calculated according to Hamilton *et al*. (1983) for an age of 550 Ma for the sediments (see item 5).

Detrital zircon grains from samples were separated using standard heavy liquid and magnetic procedures. The U-Pb analyses were performed in a multi collector SHRIMP IIe (ASI, Australia). Grains were arranged in an epoxy mount together with the Temora zircon standard (417 Ma; Black *et al*. 2003), polished to expose their cores, and covered with gold coating for internal cathodoluminescence imaging and dating. To determine the age, five scans through the mass stations were made. U concentrations were calibrated using the SL13 standard (U = 238 ppm, Williams 1998) and a

Table 1. Sm-Nd isotope data from the samples of the São Francisco Basin.

Formation	Sample	Lithology	Sm (ppm)	Nd (ppm)	$^{147}Sm/^{144}Nd$	error	$^{143}Nd/^{144}Nd$	error (2σ)	$f_{Sm/Nd}$	T_{DM} (Ga)	$\varepsilon_{Nd(550\ Ma)}$
LJ	LJ-A	Sandstone	5.705	27.838	0.1239	0.0007	0.512087	0.000004	-0.37	1.6	-5.65
LJ	FAS-LJ	Siltite	7.612	47.595	0.0967	0.0006	0.512068	0.000004	-0.51	1.3	-4.09
SSH	MG05-07	Siltite	5.699	27.634	0.1247	0.0004	0.512027	0.000008	-0.37	1.7	-6.86
SSH	MG05-11	Siltite	12.519	67.260	0.1126	0.0004	0.512072	0.000010	-0.43	1.5	-5.13
SSH	MG03-25	Siltite	5.287	22.793	0.1403	0.0005	0.512100	0.000011	-0.29	2.0	-6.54
SSH	SH-05	Sandstone	10.984	56.588	0.1174	0.0007	0.512085	0.000005	-0.40	1.5	-5.22
SSH	SH-06	Sandstone	7.351	39.624	0.1122	0.0007	0.512036	0.000004	-0.43	1.5	-5.81
SSH	MG03-24	Siltite	8.932	41.633	0.1297	0.0004	0.512081	0.000008	-0.34	1.7	-6.17
SSH	P2SH	Siltite	38.321	212.266	0.1092	0.0006	0.511926	0.000010	-0.45	1.6	-7.74
SSH	SC-SH	Siltite	12.074	61.361	0.1190	0.0007	0.512046	0.000006	-0.40	1.6	-6.10
SL CI-3	11-PGL-PEL (2)	Marlstone	1.425	7.191	0.1198	0.0007	0.511940	0.000014	-0.39	1.8	-8.22
SL CI-3	GPP-M	Marlstone	3.115	16.975	0.1110	0.0007	0.511974	0.000005	-0.44	1.6	-6.93
SL CI-2	11-VS-13 (2)	Marlstone	2.305	11.405	0.1222	0.0007	0.511967	0.000013	-0.38	1.8	-7.86
SL CI-2	11-AP-05 (2)	Sandstone	1.769	8.203	0.1304	0.0008	0.511975	0.000013	-0.34	2.0	-8.28
SL CI-2	MG05-06	Siltite	2.620	13.044	0.1215	0.0004	0.511949	0.000010	-0.38	1.8	-8.16
SL CI-2	MG05-09	Siltite	4.003	21.611	0.1120	0.0004	0.511910	0.000009	-0.43	1.7	-8.26
SL CI-2	MG05-10	Siltite	3.623	23.888	0.0917	0.0003	0.511816	0.000008	-0.53	1.5	-8.67
SL CI-2	MG05-12	Siltite	5.726	30.655	0.1129	0.0004	0.511848	0.000009	-0.43	1.8	-9.53
SL CI-2	MG05-13	Siltite	4.657	25.113	0.1121	0.0004	0.511921	0.000012	-0.43	1.7	-8.05
SL CI-2	P4	Siltite	4.509	23.368	0.1167	0.0007	0.512085	0.000007	-0.41	1.5	-5.16
SL CI-2	P5	Siltite	53.729	305.925	0.1062	0.0006	0.511930	0.000009	-0.46	1.6	-7.46
SL CI-2	FN-03	Siltite	15.050	75.968	0.1198	0.0007	0.511942	0.000008	-0.39	1.8	-8.18
SL CI-1	P6	Marlstone	5.557	27.824	0.1208	0.0007	0.511989	0.000008	-0.39	1.7	-7.33
ML	MG04-42	Claystone	8.537	39.415	0.1310	0.0004	0.511917	0.000008	-0.33	2.1	-9.46
ML	MG04-43	Claystone	7.152	36.611	0.1181	0.0004	0.511910	0.000009	-0.40	1.8	-8.69
ML	MG04-41A	Claystone	12.586	73.171	0.1040	0.0003	0.511903	0.000008	-0.47	1.6	-7.83
ML	MG03-21	Siltite	5.266	23.985	0.1328	0.0004	0.511991	0.000010	-0.33	2.0	-8.15
ML	MG03-22	Siltite	21.139	105.568	0.1211	0.0004	0.512042	0.000010	-0.38	1.6	-6.33
ML	MG03-23A	Siltite	5.353	25.762	0.1257	0.0004	0.511947	0.000011	-0.36	1.9	-8.51
ML	MG02-14B	Varvite	4.745	20.878	0.1374	0.0005	0.512010	0.000013	-0.30	2.1	-8.10
ML	MG02-11	Varvite	18.161	105.676	0.1039	0.0004	0.512018	0.000012	-0.47	1.4	-5.59
ML	MG02-13	Varvite	6.902	37.206	0.1122	0.0004	0.511918	0.000012	-0.43	1.7	-8.12
Carrancas	P12	Siltite	6.084	39.340	0.0935	0.0005	0.511843	0.000007	-0.52	1.5	-8.26
Carrancas	14-IN-CR (1)	Diamictite	10.139	54.735	0.1120	0.0007	0.511413	0.000004	-0.43	2.5	-17.98
Carrancas	MG08-04	Diamictite	1.633	9.426	0.1048	0.0006	0.511154	0.000013	-0.47	2.7	-22.52
ML	MG03-27A	Diamictite	4.169	20.818	0.1211	0.0004	0.511081	0.000011	-0.38	3.3	-25.09

ML: Moema Laminites; SL: Sete Lagoas; SSH: Serra de Santa Helena; LJ: Lagoa do Jacaré; (1) data from Guacaneme (2015); (2) data from Paula-Santos *et al.* (2015).

$^{206}Pb/^{238}U$ ratio was calibrated using the Temora standard. Decay constants used for age calculations are suggested by Steiger and Jäger (1977). The ^{204}Pb from each grain was measured for common lead correction. Squid and Isoplot programs (Ludwig 2012) were used for data processing. All obtained data were plotted on the Concordia diagram, but only ages with concordance within the 90–110% interval were used in the histograms. Ages younger than 800 Ma

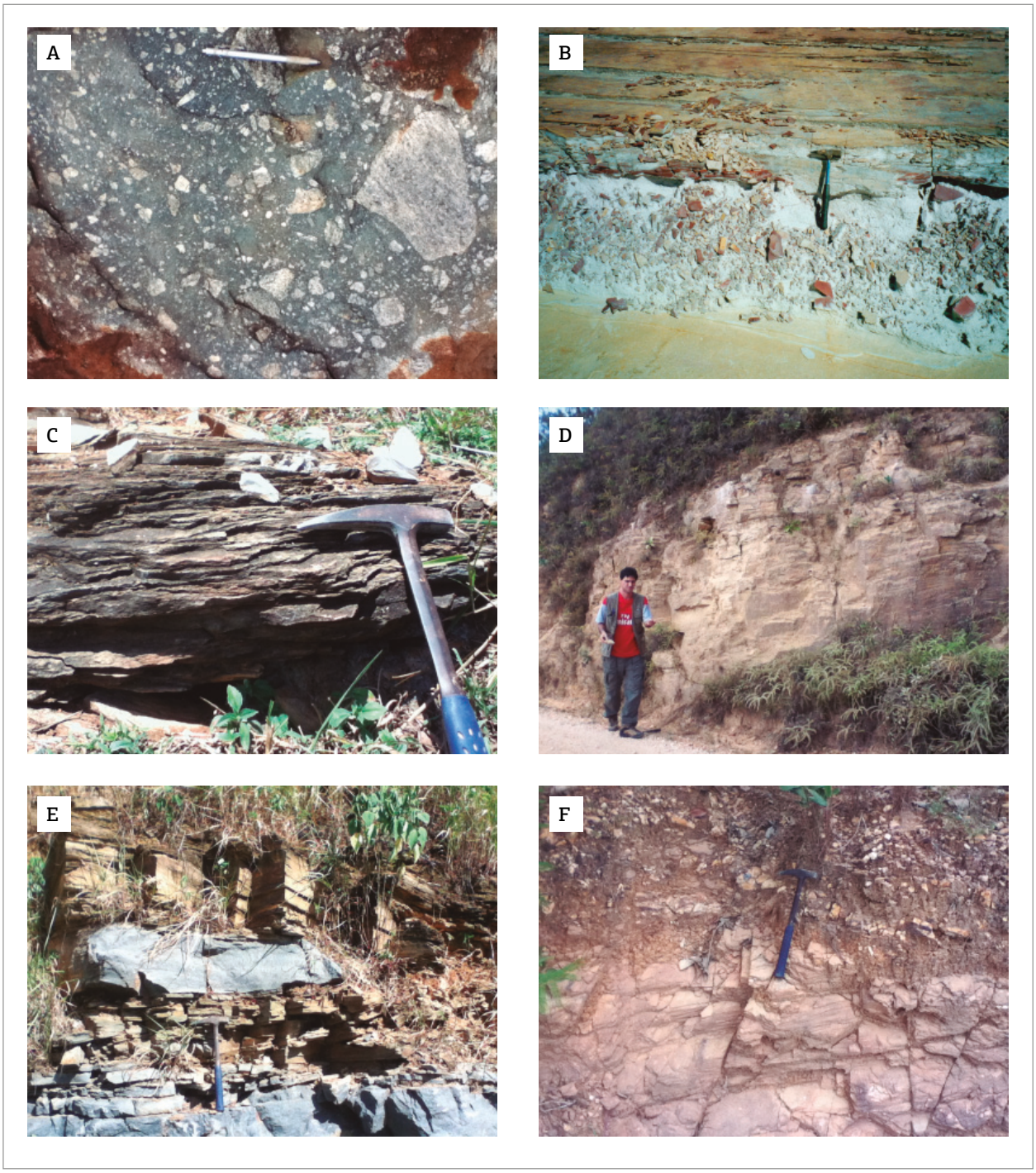

Figure 3. Field pictures showing: (A) the Carrancas Formation conglomerate in the Inhaúma city area (the pencil is 12 cm long); (B) The Moema Laminite in SAFFRAN quarry (hammer is 23 cm tall); (C) marl layer interbedded in the Sete Lagoas Formation carbonate rocks (sample GPP-M; hammer is 30 cm tall); (D) Serra de Santa Helena Formation siltites in the Lagoa Santa city area; (E) siltites and sandstones interbedded in oolithic limestones from the Lagoa do Jacaré Formation; (F) tilted siltites of the Lagoa do Jacaré Formation (sample FAS-LJ).

are referred to as $^{206}Pb/^{238}U$ ages, whereas the older ones are referred to as $^{207}Pb/^{206}Pb$ ages. Uncertainties for the measurements are reported at one sigma level.

Hf isotopic analyses were carried out in a multi collector ion coupled plasma mass spectrometer (MC-ICPMS Neptune, Thermo Fischer, Germany), which positioned spots over the ones made by SHRIMP. The average $^{176}Hf/^{177}Hf$ for the Mud Tank standard measured in the laboratory was 0.282470 ± 0.000008 (2σ, n = 85), and the average $^{176}Hf/^{177}Hf$ for the GJ standard was 0.282015 ± 0.000002 (2σ, n = 334). The initial $^{176}Hf/^{177}Hf$ (T1) ratio was calculated using the $^{206}Pb/^{238}U$ ages that were previously obtained by SHRIMP. The decay constant $^{176}Lu = 1.867 \times 10^{-11}$ yr^{-1} of Söderlund *et al.* (2004) was used. Present chondrite ratios were $^{176}Hf/^{177}Hf = 0.282772$ and $^{176}Lu/^{177}Hf = 0.0332$ (Blichert-Toft & Albarède 1997), and present day depleted mantle ratios were $^{176}Hf/^{177}Hf = 0.283225$ and $^{176}Lu/^{177}Hf = 0.038512$ (Vervoot & Blichert-Toft 1999). Model ages (TDM) were calculated using a two stage model at average crustal $^{176}Lu/^{177}Hf = 0.015$ (Griffin *et al.* 2002).

RESULTS

Sm-Nd isotope data

Table 1 exhibits the Sm-Nd isotopic results. The conglomerate samples from the Carrancas Formation yielded the oldest Sm-Nd T_{DM} ages: 2.7 and 3.3 Ga (Tab. 1; Fig. 4) in samples MG08-04 and MG03-27A, respectively. The $\varepsilon_{Nd(550\ Ma)}$ values of these rocks are also the most negative, -25.09 and -17.98 for the respective samples above, suggesting sources of long crustal residence time. These values are consistent with the data reported by Guacaneme (2015) for a conglomerate of the same unit in the Inhaúma city area (Tab. 1). The author

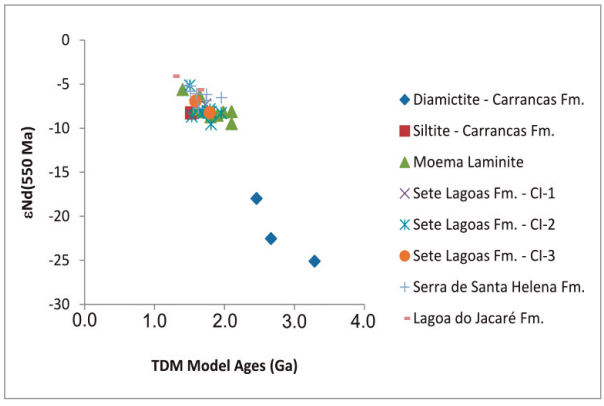

Figure 4. Sm-Nd T_{DM} ages *vs.* $\varepsilon Nd_{(550\ Ma)}$ plots of the São Francisco Basin rocks. Data were obtained from this work, Guacaneme (2015), and Paula-Santos *et al.* (2015).

obtained a Sm-Nd T_{DM} age of 2.5 Ga and an $\varepsilon_{Nd(550\ Ma)}$ value of -23.90. The transition to the siltite facies of the unit is marked by an abrupt shift to a younger age (Fig. 4). Sample P12 displays a Sm-Nd T_{DM} age of 1.5 Ga and an $\varepsilon_{Nd(550\ Ma)}$ value of -8.26. Although sources of long crustal residence were still active, contribution from younger rocks is more important in the fine-grained facies. The Moema Laminite fine-grained rocks also have model ages that are considerably younger than the conglomerates. The Sm-Nd T_{DM} ages vary from 1.4 to 2.1 Ga with $\varepsilon_{Nd(550\ Ma)}$ values between -9.46 and -5.59 (Tab. 1).

Overall, the samples from the overlying Bambuí Group yielded Sm-Nd isotopic results that were similar to the fine-grained sediments from the Carrancas Formation and the Moema Laminites (Fig. 4). The Sm-Nd T_{DM} ages are within the 1.3-2.0 Ga interval and the $\varepsilon_{Nd(550\ Ma)}$ values range from -9.53 to -4.09 (Tab. 1), which also suggests sources of long crustal residence time. The marl sample from the basal CI-1 of the Sete Lagoas Formation has a model age of 1.7 Ga. Obtained ages for the CI-2 are within the 1.5–1.8 Ga interval, which is younger than the ages obtained for the same CI by Paula-Santos *et al.* (2015; 1.8–2.0 Ga) in the south-eastern limit of the São Francisco Basin. The marlstone sample (GPP-M) of the upper CI-3 has model ages of 1.6 Ga, which is also younger than the one obtained by those authors (1.8 Ga). The Serra de Santa Helena Formation rocks yielded Sm-Nd T_{DM} ages between 1.5–2.0 Ga and the Lagoa do Jacaré Formation samples FAS-LJ and LJ-A have Sm-Nd T_{DM} ages of 1.3 and 1.6 Ga, respectively. The average of the $\varepsilon_{Nd(550\ Ma)}$ values for the Sete Lagoas Formation is slightly more negative than the average from the combined Serra de Santa Helena and Lagoa do Jacaré formations: -7.85 and -5.93, respectively.

U-Pb ages and Hf isotope data of detrital zircons

Attempts to retrieve detrital zircon grains from the samples were made, but only four samples provided enough minerals for U-Pb and Hf isotope provenance studies:

1. GPP-M from the upper Sete Lagoas Formation (CI-3, Tab. 2);
2. P2SH from the Serra de Santa Helena Formation (Tab. 3);
3. FAS-LJ (Tab. 4);
4. LJ-A (Tab. 5), both from the Lagoa do Jacaré Formation.

Only samples P2SH and FAS-LJ provided more than 30 zircon grains within a 90–110% concordance range. Therefore, the calculation of the zircon population probability was performed for only these samples. The Hf isotope data was obtained for the Late Cryogenian / Early Ediacaran grains from sample P2SH as an effort to track the sources of the zircons (Tab. 6).

Table 2. U-Pb isotope data by SHRIMP in detrital zircon grains from sample GPP-M (Sete Lagoas Formation).

						Radiogenic ratios						r	Age (Ma)				
Grain. spot	U (ppm)	Th (ppm)	Th/U	$^{206}Pb^*$ (ppm)	f_{206} %	$^{206}Pb/^{238}U$	±	$^{207}Pb/^{235}U$	±	$^{207}Pb/^{206}Pb$	±		$^{206}Pb/^{238}U$	±	$^{207}Pb/^{206}Pb$	±	% Disc
1.1	392	1384	3.65	35	2.25	0.1009	0.0171	0.8485	0.0594	0.0610	0.0556	0.29	619	10	640	122	3
2.1	497	161	0.34	55	2.84	0.1248	0.0183	1.0951	0.0669	0.0637	0.0622	0.27	758	13	730	136	-4
3.1	503	81	0.17	96	2.19	0.2163	0.0182	4.0649	0.0312	0.1362	0.0242	0.58	1262	21	2181	44	73
4.1	873	158	0.19	381	0.01	0.5074	0.0192	9.4476	0.0205	0.1350	0.0072	0.94	2646	42	2165	13	-18
5.1	404	93	0.24	60	0.62	0.1730	0.0165	2.8239	0.0193	0.1184	0.0098	0.85	1028	16	1932	18	88
6.1	543	288	0.55	53	0.26	0.1136	0.0168	0.9599	0.0230	0.0613	0.0156	0.73	693	11	650	34	-6
7.1	472	316	0.69	48	1.87	0.1148	0.0165	1.2936	0.0366	0.0817	0.0317	0.45	701	11	1238	64	77
8.1	466	56	0.12	157	0.10	0.3911	0.0165	6.7984	0.0171	0.1261	0.0044	0.97	2128	30	2044	8	-4
9.1	285	259	0.94	94	1.78	0.3755	0.0169	6.4874	0.0303	0.1253	0.0231	0.56	2055	30	2033	44	-1
10.1	224	150	0.69	64	0.07	0.3298	0.0173	4.6345	0.0203	0.1019	0.0105	0.85	1837	28	1660	20	-10
11.1	333	595	1.85	87	1.08	0.2993	0.0167	5.7306	0.0208	0.1388	0.0117	0.80	1688	25	2213	22	31
12.1	339	98	0.30	103	0.15	0.3530	0.0165	8.3649	0.0170	0.1719	0.0041	0.97	1949	28	2576	7	32
13.1	275	95	0.36	128	0.14	0.5405	0.0175	14.2720	0.0178	0.1915	0.0032	0.98	2785	40	2755	5	-1
14.1	491	267	0.56	61	2.45	0.1408	0.0168	1.2865	0.0552	0.0663	0.0506	0.30	849	13	814	110	-4
15.1	433	105	0.25	37	0.77	0.0988	0.0165	0.9428	0.0269	0.0692	0.0211	0.61	607	10	906	44	49
16.1	620	526	0.88	68	0.01	0.1270	0.0175	1.1548	0.0186	0.0660	0.0063	0.94	771	13	805	13	5
17.1	139	75	0.56	44	0.63	0.3630	0.0172	6.4702	0.0204	0.1293	0.0105	0.84	1996	30	2088	19	5
18.1	407	62	0.16	48	1.40	0.1350	0.0166	1.3041	0.0345	0.0700	0.0294	0.48	817	13	930	62	14
19.1	272	63	0.24	77	0.32	0.3271	0.0168	7.8144	0.0176	0.1732	0.0052	0.95	1824	27	2590	9	42
20.1	447	67	0.16	74	0.77	0.1903	0.0164	3.6148	0.0194	0.1377	0.0100	0.85	1123	17	2199	18	96
21.1	316	337	1.10	61	2.86	0.2171	0.0180	2.3765	0.0719	0.0794	0.0672	0.25	1266	21	1182	138	-7
22.1	196	350	1.85	32	2.99	0.1835	0.0186	1.8725	0.0843	0.0740	0.0799	0.22	1086	18	1042	166	-4
23.1	311	239	0.79	61	1.30	0.2239	0.0173	2.5011	0.0355	0.0810	0.0300	0.49	1303	20	1222	61	-6
25.1	305	148	0.50	69	1.70	0.2572	0.0167	4.7220	0.0253	0.1331	0.0178	0.66	1475	22	2140	33	45
26.1	878	408	0.48	267	0.04	0.3539	0.0162	6.5808	0.0164	0.1349	0.0024	0.99	1953	27	2162	4	11
27.1	509	213	0.43	61	1.31	0.1372	0.0164	2.1228	0.0242	0.1122	0.0173	0.68	829	13	1835	32	121
28.1	369	447	1.25	32	4.39	0.0949	0.0173	0.7808	0.1034	0.0597	0.0991	0.17	584	10	592	221	1
29.1	515	85	0.17	159	0.07	0.3603	0.0165	6.1044	0.0169	0.1229	0.0038	0.97	1984	28	1998	7	1
30.1	450	193	0.44	149	0.07	0.3856	0.0164	7.4182	0.0173	0.1395	0.0055	0.95	2102	29	2221	10	6
31.1	353	74	0.22	129	0.06	0.4245	0.0168	7.4713	0.0173	0.1277	0.0044	0.97	2281	32	2066	8	-9
32.1	110	79	0.74	46	0.53	0.4851	0.0173	12.5233	0.0189	0.1872	0.0071	0.92	2550	37	2718	12	7
33.1	251	123	0.50	102	0.32	0.4719	0.0176	11.2107	0.0186	0.1723	0.0059	0.95	2492	36	2580	10	4

The errors are at 1-sigma level.

Table 3. U-Pb isotope data by SHRIMP in detrital zircon grains from sample P2SH (Serra de Santa Helena Formation).

						Radiogenic ratios						r	Age (Ma)				%
Grain.	U	Th	Th/U	$^{206}Pb^*$	f_{206}	$^{206}Pb/$	±	$^{207}Pb/$	±	$^{207}Pb/$	±		$^{206}Pb/$	±	$^{207}Pb/$	±	
spot	(ppm)	(ppm)		(ppm)	%	^{238}U		^{235}U		^{206}Pb			^{238}U		^{206}Pb		Disc
1.1	311	581	1.93	28	1.66	0.1014	0.0499	0.8475	0.0702	0.0606	0.0486	0.71	623	30	625	106	0
2.1	317	319	1.04	29	0.44	0.1073	0.0498	0.9166	0.0551	0.0619	0.0235	0.90	657	31	672	50	2
3.1	349	768	2.27	30	1.49	0.0982	0.0494	0.8211	0.0679	0.0607	0.0458	0.73	604	29	627	100	4
4.1	192	110	0.59	18	0.60	0.1077	0.0496	0.8929	0.0576	0.0601	0.0291	0.86	660	31	607	63	-8
5.1	277	367	1.37	24	1.22	0.1008	0.0495	0.8451	0.0632	0.0608	0.0387	0.78	619	29	632	85	2
6.1	247	841	3.52	20	3.59	0.0922	0.0500	0.9111	0.1018	0.0716	0.0872	0.49	569	27	976	181	72
7.1	345	585	1.75	27	0.71	0.0919	0.0494	0.7733	0.0563	0.0610	0.0267	0.88	567	27	640	58	13
8.1	371	430	1.20	33	1.72	0.1027	0.0494	0.8566	0.0696	0.0605	0.0482	0.71	630	30	621	106	-1
9.1	618	765	1.28	75	0.09	0.1415	0.0497	1.2698	0.0524	0.0651	0.0166	0.95	853	40	778	35	-9
10.1	427	260	0.63	38	0.38	0.1035	0.0493	0.8619	0.0528	0.0604	0.0186	0.93	635	30	618	40	-3
11.1	401	1254	3.23	35	2.25	0.0995	0.0496	0.8518	0.0811	0.0621	0.0631	0.61	611	29	677	137	11
12.1	566	715	1.30	49	1.09	0.0990	0.0493	0.8131	0.0579	0.0596	0.0298	0.85	608	29	589	66	-3
13.1	207	148	0.74	19	0.18	0.1057	0.0495	0.8636	0.0529	0.0593	0.0186	0.94	648	31	576	40	-11
14.1	285	185	0.67	26	0.12	0.1055	0.0495	0.8822	0.0511	0.0607	0.0128	0.97	646	30	627	28	-3
15.1	525	742	1.46	46	1.06	0.1002	0.0493	0.8798	0.0597	0.0637	0.0332	0.83	616	29	731	71	19
16.1	378	509	1.39	33	1.33	0.0998	0.0494	0.8400	0.0629	0.0611	0.0383	0.79	613	29	642	84	5
17.1	303	342	1.17	26	0.25	0.0995	0.0494	0.8244	0.0539	0.0601	0.0217	0.92	611	29	608	47	-1
18.1	366	351	0.99	33	0.13	0.1055	0.0494	0.8853	0.0520	0.0609	0.0163	0.95	646	30	635	35	-2
19.1	315	254	0.83	27	0.59	0.0989	0.0500	0.8295	0.0589	0.0608	0.0309	0.85	608	29	634	67	4
20.1	360	742	2.13	37	1.18	0.1193	0.0495	1.0396	0.0635	0.0632	0.0393	0.78	726	34	716	85	-1
21.1	651	517	0.82	62	1.49	0.1089	0.0500	0.9274	0.0658	0.0618	0.0421	0.76	666	32	666	92	0
22.1	300	198	0.68	27	0.12	0.1038	0.0494	0.8670	0.0515	0.0606	0.0146	0.96	636	30	625	31	-2
23.1	343	390	1.17	30	0.33	0.1027	0.0494	0.8803	0.0527	0.0622	0.0185	0.94	630	30	680	40	8
24.1	274	374	1.41	25	1.12	0.1031	0.0495	0.8786	0.0612	0.0618	0.0356	0.81	633	30	667	77	5
25.1	473	1346	2.94	37	2.69	0.0886	0.0495	0.7399	0.0925	0.0606	0.0769	0.54	547	26	623	168	14
26.1	223	161	0.74	20	0.50	0.1030	0.0495	0.8380	0.0560	0.0590	0.0260	0.88	632	30	567	57	-10
27.1	503	351	0.72	45	0.43	0.1029	0.0494	0.8498	0.0535	0.0599	0.0204	0.92	631	30	600	44	-5
28.1	322	621	1.99	26	3.32	0.0902	0.0497	0.7564	0.0988	0.0609	0.0836	0.50	557	27	634	184	14
29.1	296	197	0.69	29	0.36	0.1144	0.0495	0.9720	0.0558	0.0616	0.0257	0.89	698	33	662	55	-5
30.1	373	929	2.58	34	2.15	0.1049	0.0495	0.9019	0.0779	0.0624	0.0590	0.64	643	30	686	128	7
31.1	150	154	1.06	13	0.98	0.1033	0.0500	0.8745	0.0715	0.0614	0.0508	0.70	634	30	654	110	3
32.1	349	255	0.75	32	0.79	0.1056	0.0495	0.8829	0.0606	0.0607	0.0346	0.82	647	30	627	75	-3
33.1	305	230	0.78	28	0.25	0.1080	0.0495	0.8990	0.0531	0.0604	0.0191	0.93	661	31	616	41	-7
34.1	317	809	2.64	20	4.83	0.0713	0.0501	0.6006	0.1374	0.0611	0.1259	0.36	444	21	644	275	45
35.1	165	147	0.92	15	0.63	0.1042	0.0498	0.8723	0.0554	0.0607	0.0241	0.90	639	30	629	52	-2
36.1	338	377	1.15	29	1.19	0.0980	0.0495	0.8131	0.0642	0.0602	0.0405	0.77	603	28	609	89	1
37.1	450	591	1.36	40	0.77	0.1015	0.0494	0.8467	0.0573	0.0605	0.0286	0.86	623	29	622	62	0
38.1	179	214	1.24	16	0.65	0.1053	0.0497	0.8923	0.0586	0.0614	0.0309	0.85	645	31	655	67	1
39.1	273	273	1.04	26	1.50	0.1092	0.0495	0.9330	0.0698	0.0620	0.0486	0.71	668	31	674	105	1

The errors are at 1-sigma level.

Table 4. U-Pb isotope data by SHRIMP in detrital zircon grains from sample FAS-LJ (Lagoa do Jacaré Formation).

						Radiogenic ratios						r	Age (Ma)				%
Grain. spot	U (ppm)	Th (ppm)	Th/U	$^{206}Pb^*$ (ppm)	f_{206} %	$^{206}Pb/^{238}U$	±	$^{207}Pb/^{235}U$	±	$^{207}Pb/^{206}Pb$	±		$^{206}Pb/^{238}U$	±	$^{207}Pb/^{206}Pb$	±	Disc
1.1	326	115	0.36	52	1.23	0.1836	0.0168	1.9197	0.0321	0.0758	0.0265	0.52	1087	17	1090	55	0
2.1	158	151	0.99	16	4.98	0.1107	0.0207	0.9538	0.1278	0.0625	0.1227	0.16	677	13	692	269	2
3.1	220	214	1.00	19	5.21	0.0939	0.0186	0.7773	0.1361	0.0600	0.1316	0.14	579	10	604	292	4
4.1	185	225	1.26	17	2.45	0.1070	0.0181	0.9515	0.0746	0.0645	0.0712	0.24	655	11	758	153	16
5.1	307	255	0.86	32	1.44	0.1186	0.0171	1.0316	0.0453	0.0631	0.0412	0.38	722	12	711	89	-2
6.1	104	43	0.42	43	<LD	0.4844	0.0173	9.0651	0.0186	0.1357	0.0069	0.93	2547	36	2173	12	-15
7.1	278	300	1.12	39	2.72	0.1598	0.0173	1.5334	0.0615	0.0696	0.0568	0.28	956	15	916	121	-4
8.1	348	93	0.28	38	0.89	0.1267	0.0169	1.1637	0.0331	0.0666	0.0281	0.51	769	12	826	59	8
9.1	176	107	0.63	15	0.36	0.0995	0.0176	0.8472	0.0325	0.0617	0.0273	0.54	612	10	665	59	9
10.1	137	176	1.33	38	0.80	0.3166	0.0174	5.2151	0.0230	0.1195	0.0145	0.76	1773	27	1948	27	10
11.1	142	144	1.05	18	2.91	0.1401	0.0182	1.2680	0.0789	0.0657	0.0747	0.23	845	14	795	161	-6
12.1	176	150	0.88	31	1.88	0.2005	0.0180	2.0913	0.0573	0.0756	0.0531	0.31	1178	19	1085	109	-8
13.1	281	140	0.52	25	4.07	0.1005	0.0176	0.8593	0.0993	0.0620	0.0953	0.18	617	10	674	209	9
14.1	334	370	1.14	28	2.98	0.0940	0.0171	0.7954	0.0720	0.0613	0.0683	0.24	579	9	651	150	12
15.1	274	79	0.30	27	0.90	0.1132	0.0175	0.9853	0.0417	0.0631	0.0375	0.42	691	11	712	80	3
16.1	447	257	0.59	57	0.35	0.1466	0.0166	1.3548	0.0213	0.0670	0.0132	0.78	882	14	838	28	-5
17.1	239	135	0.58	32	3.55	0.1500	0.0219	1.4254	0.0863	0.0689	0.0807	0.25	901	18	896	172	-1
18.1	243	242	1.03	36	0.19	0.1718	0.0168	1.6973	0.0212	0.0717	0.0128	0.79	1022	16	976	26	-4
19.1	796	193	0.25	187	0.24	0.2729	0.0163	4.1912	0.0169	0.1114	0.0043	0.96	1556	22	1822	8	17
20.1	541	181	0.35	85	2.68	0.1766	0.0171	1.7530	0.0621	0.0720	0.0574	0.28	1048	17	986	122	-6
21.1	174	120	0.71	37	2.01	0.2444	0.0173	3.2693	0.0390	0.0970	0.0332	0.44	1409	22	1568	66	11
22.1	336	336	1.03	32	6.11	0.1044	0.0179	0.8769	0.1407	0.0610	0.1350	0.13	640	11	637	300	0
23.1	169	150	0.92	19	2.47	0.1270	0.0175	1.1308	0.0653	0.0646	0.0613	0.27	771	13	761	133	-1
24.1	298	189	0.66	27	0.76	0.1036	0.0169	0.8670	0.0336	0.0607	0.0288	0.50	636	10	628	63	-1
25.1	328	782	2.46	134	0.20	0.4748	0.0170	7.4859	0.0190	0.1144	0.0083	0.89	2505	35	1870	15	-25
26.1	227	156	0.71	55	0.85	0.2816	0.0171	3.5893	0.0250	0.0925	0.0175	0.68	1599	24	1477	35	-8
27.1	417	448	1.11	70	2.34	0.1913	0.0170	1.9678	0.0563	0.0746	0.0517	0.30	1128	18	1058	108	-6
28.1	95	131	1.42	18	1.70	0.2125	0.0211	2.3270	0.0475	0.0794	0.0413	0.44	1242	24	1183	84	-5
29.1	93	74	0.82	15	5.76	0.1735	0.0206	1.8271	0.1324	0.0764	0.1257	0.16	1031	19	1105	261	7
30.1	176	68	0.40	85	0.39	0.5592	0.0172	15.4520	0.0196	0.2004	0.0092	0.88	2863	40	2829	15	-1
31.1	222	121	0.56	31	1.48	0.1609	0.0174	1.5233	0.0444	0.0687	0.0398	0.39	962	16	889	84	-8
32.1	299	195	0.68	85	0.61	0.3272	0.0171	4.7916	0.0204	0.1062	0.0106	0.84	1825	27	1735	20	-5
33.1	326	128	0.41	35	0.63	0.1243	0.0167	1.1143	0.0274	0.0650	0.0215	0.61	755	12	776	46	3
34.1	314	65	0.21	43	0.37	0.1601	0.0166	1.5729	0.0229	0.0713	0.0155	0.73	957	15	965	32	1

Continue...

Table 4. Continuation.

						Radiogenic ratios						r	Age (Ma)				%
Grain. spot	U (ppm)	Th (ppm)	Th/U	$^{206}Pb^*$ (ppm)	f_{206} %	$^{206}Pb/^{238}U$	±	$^{207}Pb/^{235}U$	±	$^{207}Pb/^{206}Pb$	±		$^{206}Pb/^{238}U$	±	$^{207}Pb/^{206}Pb$	±	Disc
35.1	309	91	0.31	44	0.70	0.1642	0.0167	1.5939	0.0259	0.0704	0.0194	0.64	980	15	940	41	-4
36.1	346	176	0.52	198	0.06	0.6659	0.0169	18.6449	0.0173	0.2031	0.0037	0.98	3290	43	2851	6	-13
37.1	252	230	0.95	31	2.33	0.1400	0.0176	1.3654	0.0628	0.0707	0.0590	0.28	845	14	950	123	12
38.1	363	528	1.50	33	1.46	0.1044	0.0168	0.8972	0.0417	0.0623	0.0374	0.40	640	10	685	82	7
39.1	198	121	0.63	31	2.03	0.1791	0.0197	1.8074	0.0555	0.0732	0.0504	0.35	1062	19	1019	105	-4
40.1	552	401	0.75	86	1.87	0.1771	0.0241	1.8569	0.0450	0.0761	0.0365	0.54	1051	23	1096	76	4
41.1	207	183	0.91	31	0.46	0.1714	0.0172	1.6833	0.0237	0.0712	0.0161	0.72	1020	16	964	33	-6
42.1	428	199	0.48	75	0.19	0.2031	0.0164	2.2623	0.0181	0.0808	0.0074	0.91	1192	18	1217	15	2
43.1	202	133	0.68	21	1.35	0.1218	0.0174	1.0821	0.0500	0.0644	0.0462	0.35	741	12	755	99	2
44.1	413	183	0.46	191	0.37	0.5339	0.0164	13.2300	0.0171	0.1797	0.0044	0.96	2758	37	2650	8	-4
45.1	225	99	0.46	65	1.32	0.3297	0.0169	5.3416	0.0249	0.1175	0.0169	0.68	1837	27	1919	33	4
46.1	152	76	0.52	22	1.00	0.1652	0.0175	1.6662	0.0379	0.0732	0.0331	0.46	985	16	1018	68	3
47.1	259	94	0.37	30	1.68	0.1322	0.0171	1.1624	0.0476	0.0638	0.0433	0.36	800	13	734	94	-8
48.1	297	115	0.40	54	0.27	0.2097	0.0171	2.2324	0.0223	0.0772	0.0143	0.76	1227	19	1127	29	-8
49.1	404	275	0.70	272	0.06	0.7808	0.0167	28.3959	0.0173	0.2638	0.0045	0.97	3720	47	3269	7	-12
50.1	372	182	0.51	48	2.63	0.1448	0.0173	1.3439	0.0649	0.0673	0.0606	0.27	872	14	847	130	-3
51.1	163	54	0.34	16	2.35	0.1119	0.0179	0.9422	0.0724	0.0611	0.0689	0.25	684	12	642	151	-6
52.1	363	311	0.88	65	1.68	0.2054	0.0170	2.1943	0.0403	0.0775	0.0350	0.42	1204	19	1134	73	-6

The errors are at 1-sigma level; <LD: below detection limit.

Additionally, eleven grains from sample P12 of the Carrancas Formation were dated, but only six of the ages were within the concordance range (Tab. 7). The remaining five grains yielded discordant ages and high common lead concentrations. The concordant U-Pb ages vary from 1922 to 485 Ma.

Sample GPP-M provided colourless subeuhedral and reddish rounded grains with the largest side sizes ranging from 80 to 200 µm and igneous oscillatory zoning (Fig. 5). Thirty-two grains were analysed, but twenty-two of them yielded high common lead concentrations and high analytical errors. Only eleven grains yielded ages within the 90–110% concordance range (Tab. 2). The Concordia diagram (Fig. 6A) show age concentrations at 800, 1200 and 2000 Ma, but two sets of grains also plot discordias with upper intercepts close to 2200 and 2800 Ma, and lower intercepts towards Neoproterozoic, suggesting Pb loss at this time.

The retrieved grains from sample P2SH are yellowish, euhedral to sub-euhedral, with the largest side of ca being 100 µm, and with igneous oscillatory zoning (Fig. 5). Thirty of the thirty-nine grains that were dated yielded low common Pb concentrations and concordant ages (Tab. 3). The U-Pb ages obtained have high analytical errors, even for the zircons with low common lead concentrations (Tab. 3), and they vary between 603 and 726 Ma. The Concordia diagrams and the age distribution histogram show a single dominant population aged around 630 Ma (Fig. 6B and Fig. 7A). A Concordia age of 631 ± 5 Ma was calculated (n = 28; Fig. 5B), and the ages older than 690 Ma were suppressed for better results. The $\varepsilon_{Hf(t)}$ values of the grains are negative and vary from -13.94 to -5.36 and the Hf T_{DM} ages are between 1.9 to 2.4 Ga (Tab. 6; Fig. 8).

Zircon grains retrieved from sample FAS-LJ (n = 52) are colourless, sub-euhedral to sub-rounded and their largest side ranges from 80 to 150 µm. The grains display mainly igneous oscillatory zoning (Fig. 5). Forty-two grains yielded concordant ages (Tab. 4). The main age populations (30% of the grains each) are dated at ca. 810 and 950 Ma

Table 5. U-Pb isotope data by SHRIMP in detrital zircon grains from sample LJ-A (Jagoa do Jacaré Formation).

						Radiogenic ratios							Age (Ma)				
Grain.	U	Th	Th/U	$^{206}Pb^*$	f_{206}	$^{206}Pb/$	±	$^{207}Pb/$		$^{207}Pb/$		r	$^{206}Pb/$	±	$^{207}Pb/$	±	%
spot	(ppm)	(ppm)		(ppm)	%	^{238}U		^{235}U	±	^{206}Pb	±		^{238}U		^{206}Pb		Disc
1.1	426	196	0.48	55	0.47	0.1506	0.0167	1.3953	0.0225	0.0672	0.0148	0.74	904	14	844	31	-7
2.1	162	265	1.69	14	0.04	0.1003	0.0174	0.8172	0.0280	0.0591	0.0219	0.62	616	10	570	48	-8
3.1	724	380	0.54	59	2.02	0.0932	0.0166	0.7841	0.0510	0.0610	0.0471	0.33	574	9	640	104	11
4.1	483	152	0.32	42	0.23	0.1017	0.0165	0.8546	0.0218	0.0609	0.0141	0.76	624	10	637	31	2
5.1	408	442	1.12	38	1.65	0.1055	0.0175	0.8657	0.0471	0.0596	0.0428	0.37	646	11	587	95	-9
6.1	407	164	0.42	56	1.15	0.1587	0.0168	1.5556	0.0333	0.0711	0.0280	0.50	950	15	959	59	1
7.1	214	114	0.55	30	0.54	0.1593	0.0171	1.5446	0.0273	0.0703	0.0211	0.63	953	15	938	44	-2
8.1	490	92	0.19	120	0.07	0.2843	0.0164	4.6829	0.0168	0.1195	0.0038	0.97	1.613	23	1948	7	21
9.1	211	238	1.17	21	2.36	0.1108	0.0178	0.9325	0.0703	0.0610	0.0667	0.25	678	11	640	146	-6
10.1	265	167	0.65	26	1.31	0.1105	0.0171	0.9304	0.0514	0.0611	0.0479	0.33	675	11	642	104	-5
11.1	288	104	0.37	60	0.07	0.2425	0.0167	2.9958	0.0176	0.0896	0.0057	0.95	1.400	21	1417	11	1
12.1	269	87	0.33	37	0.25	0.1603	0.0168	1.5501	0.0207	0.0701	0.0120	0.81	958	15	932	25	-3
13.1	574	379	0.68	56	0.29	0.1133	0.0165	0.9794	0.0210	0.0627	0.0130	0.78	692	11	698	28	1
14.1	257	141	0.57	29	1.40	0.1301	0.0172	1.1762	0.0434	0.0656	0.0391	0.40	788	13	793	84	1
15.1	279	145	0.54	29	0.97	0.1209	0.0174	1.0541	0.0439	0.0632	0.0399	0.40	736	12	715	86	-3
16.1	436	978	2.32	39	2.45	0.1005	0.0170	0.8425	0.0603	0.0608	0.0563	0.28	618	10	631	124	2
17.1	962	395	0.42	129	3.35	0.1504	0.0219	1.6299	0.1071	0.0786	0.1032	0.20	903	18	1162	208	29
18.1	516	172	0.34	50	1.18	0.1107	0.0167	0.9261	0.0365	0.0607	0.0318	0.46	677	11	627	70	-7
19.1	144	117	0.84	12	1.03	0.0969	0.0176	0.7901	0.0483	0.0591	0.0446	0.36	596	10	572	98	-4
20.1	350	285	0.84	40	0.72	0.1333	0.0167	1.2046	0.0558	0.0655	0.0530	0.30	807	13	792	112	-2
21.1	647	345	0.55	104	3.38	0.1809	0.0200	1.8906	0.1064	0.0758	0.1023	0.19	1.072	20	1089	209	2
22.1	112	35	0.32	15	0.40	0.1526	0.0178	1.4413	0.0315	0.0685	0.0259	0.56	916	15	883	54	-4
23.1	380	92	0.25	44	1.25	0.1317	0.0168	1.1820	0.0361	0.0651	0.0312	0.46	798	13	777	67	-3
24.1	672	283	0.43	82	0.58	0.1406	0.0164	1.3341	0.0223	0.0688	0.0147	0.74	848	13	894	31	5
25.1	1084	156	0.15	146	0.23	0.1559	0.0164	1.4579	0.0200	0.0678	0.0113	0.82	934	14	864	24	-7
26.1	215	73	0.35	78	0.30	0.4225	0.0170	7.7580	0.0185	0.1332	0.0072	0.92	2.272	32	2140	13	-6
27.1	659	1026	1.61	51	2.42	0.0878	0.0172	0.7429	0.0587	0.0614	0.0548	0.29	543	9	652	120	20
28.1	296	214	0.75	34	9.07	0.1223	0.0212	1.0461	0.2105	0.0621	0.2007	0.10	744	15	676	448	-9
29.1	336	101	0.31	45	2.02	0.1516	0.0168	1.4646	0.0470	0.0701	0.0423	0.36	910	14	930	90	2
30.1	660	278	0.43	59	3.43	0.1002	0.0172	0.8227	0.0791	0.0595	0.0749	0.22	616	10	587	168	-5
31.1	345	82	0.24	40	1.05	0.1340	0.0168	1.2306	0.0344	0.0666	0.0294	0.49	811	13	825	63	2
32.1	669	453	0.70	67	1.91	0.1144	0.0166	1.0261	0.0445	0.0651	0.0401	0.37	698	11	776	87	11
33.1	788	194	0.25	83	2.87	0.1193	0.0169	1.0551	0.0684	0.0641	0.0644	0.25	727	12	746	140	3
34.1	553	258	0.48	51	3.35	0.1046	0.0203	0.9025	0.0824	0.0626	0.0778	0.25	641	12	695	170	8
35.1	528	30	0.06	183	0.09	0.4025	0.0180	9.8916	0.0182	0.1782	0.0027	0.99	2.181	33	2636	5	21

The errors are at 1-sigma level.

(Fig. 6C and Fig. 7B). Two populations between 1100 and 1200 Ma are defined by 20% of the grains. Minor populations (< 5%) are dated between 1400 and 2200 Ma and four grains displayed Archean ages.

Sample LJ-A provided mainly euhedral to subeuhedral colourless zircons with the largest side ranging from 70 to 250 µm (n = 35; Fig. 5). Concordant zircon grains (n = 29) are dated between 600 and 1100 Ma (Fig. 6D).

DISCUSSION

Sedimentary Provenance and tectonic implications

Our Sm-Nd data suggest little variation in the sedimentary sources active during the deposition of most of the basal glaciogenic units and the Bambuí Group

Table 6. Hf isotope data obtained by LA-ICPMS in the detrital zircons from sample P2SH (Serra de Santa Helena Formation).

Spot	$^{176}Hf/^{177}Hf$	±	$^{176}Lu/^{177}Hf$	±	U-Pb Age	ε Hf(0)	$^{176}Hf/^{177}Hf$	ε Hf	$^{176}Hf/^{177}Hf$	T DM	$^{176}Hf/^{177}Hf$	ε Hf
					(T1) Ma		(T1)	(T1)	DM(T)*	(Ma)	DM(T)**	(TDM)
1.1	0.282016	0.000055	0.002194	0.000013	623	-26.7	0.281990	-13.9	0.282774	2389	0.281469	7.5
2.1	0.282025	0.000033	0.001417	0.000021	657	-26.4	0.282007	-12.6	0.282750	2330	0.281513	7.7
8.1	0.282023	0.000042	0.001648	0.000005	630	-26.5	0.282003	-13.3	0.282769	2355	0.281494	7.6
17.1	0.282171	0.000030	0.001302	0.000017	611	-21.2	0.282156	-8.3	0.282783	2027	0.281740	8.8
20.1	0.282122	0.000037	0.002064	0.000026	726	-23.0	0.282094	-8.0	0.282699	2094	0.281690	8.6
21.1	0.282106	0.000034	0.002165	0.000058	666	-23.5	0.282079	-9.8	0.282743	2165	0.281637	8.3
35.1	0.282092	0.000035	0.001145	0.000022	639	-24.1	0.282078	-10.5	0.282763	2184	0.281623	8.3
36.1	0.282090	0.000028	0.001896	0.000026	602	-24.1	0.282069	-11.6	0.282790	2227	0.281590	8.1
37.1	0.282116	0.000030	0.001047	0.000004	623	-23.2	0.282104	-9.9	0.282774	2136	0.281658	8.4
38.1	0.282234	0.000039	0.002211	0.000043	600	-19.0	0.282209	-6.7	0.282791	1915	0.281823	9.2
39.1	0.282238	0.000027	0.001599	0.000023	645	-18.9	0.282219	-5.4	0.282758	1867	0.281860	9.4

Errors are at 2-sigma level; *single stage; **double stage.

Table 7. U-Pb isotope data by SHRIMP in detrital zircon grains from sample P12 (Carrancas Formation).

						Radiogenic ratios						r	Age (Ma)				%
Grain.	U	Th	Th/U	$^{206}Pb^*$	f_{206}	$^{206}Pb/$	±	$^{207}Pb/$	±	$^{207}Pb/$	±		$^{206}Pb/$	±	$^{207}Pb/$	±	
spot	(ppm)	(ppm)		(ppm)	%	^{238}U		^{235}U		^{206}Pb			^{238}U		^{206}Pb		Disc
1.1	242	165	0.71	20	<LD	0.0986	0.0209	0.8190	0.0321	0.0602	0.0244	0.65	606	12	611	53	1
2.1	414	101	0.25	110	0.05	0.3093	0.0202	4.6204	0.0281	0.1083	0.0195	0.72	1737	31	1771	36	2
3.1	395	71	0.19	115	0.59	0.3362	0.0206	7.3438	0.0233	0.1584	0.0107	0.88	1868	33	2439	19	31
4.1	472	176	0.38	52	0.84	0.1267	0.0203	2.1173	0.0273	0.1212	0.0182	0.74	769	15	1974	33	157
5.1	132	141	1.10	39	0.12	0.3473	0.0253	5.5632	0.0263	0.1162	0.0072	0.96	1922	42	1898	13	-1
6.1	309	412	1.38	28	0.31	0.1061	0.0206	0.9304	0.0240	0.0636	0.0121	0.86	650	13	729	26	12
7.1	327	186	0.59	27	0.27	0.0970	0.0204	0.7934	0.0261	0.0593	0.0162	0.78	597	12	578	35	-3
8.1	372	179	0.50	25	<LD	0.0781	0.0210	0.6094	0.0253	0.0566	0.0141	0.83	485	10	475	31	-2
9.1	468	63	0.14	43	0.67	0.1067	0.0202	1.3362	0.0250	0.0908	0.0145	0.81	654	13	1442	28	121
10.1	138	126	0.94	18	<LD	0.1553	0.0237	1.6014	0.0262	0.0748	0.0112	0.90	931	21	1063	23	14
11.1	106	116	1.12	28	0.10	0.3102	0.0216	4.6544	0.0236	0.1088	0.0095	0.92	1742	33	1780	17	2

The errors are at 1-sigma level; <LD: below detection limit.

(Fig. 4). The exception is the conglomeratic facies of the Carrancas Formation, which yielded Archean T_{DM} ages (Tab. 1). Although the abrupt shift in the ages between the coarser and finer sediments could suggest a possible unconformity in the lower portion of the São Francisco Basin, it may occur due to a change in the basin sediment

Figure 5. Cathodoluminescence images of the detrital zircon grains retrieved from samples of the Bambuí Group.

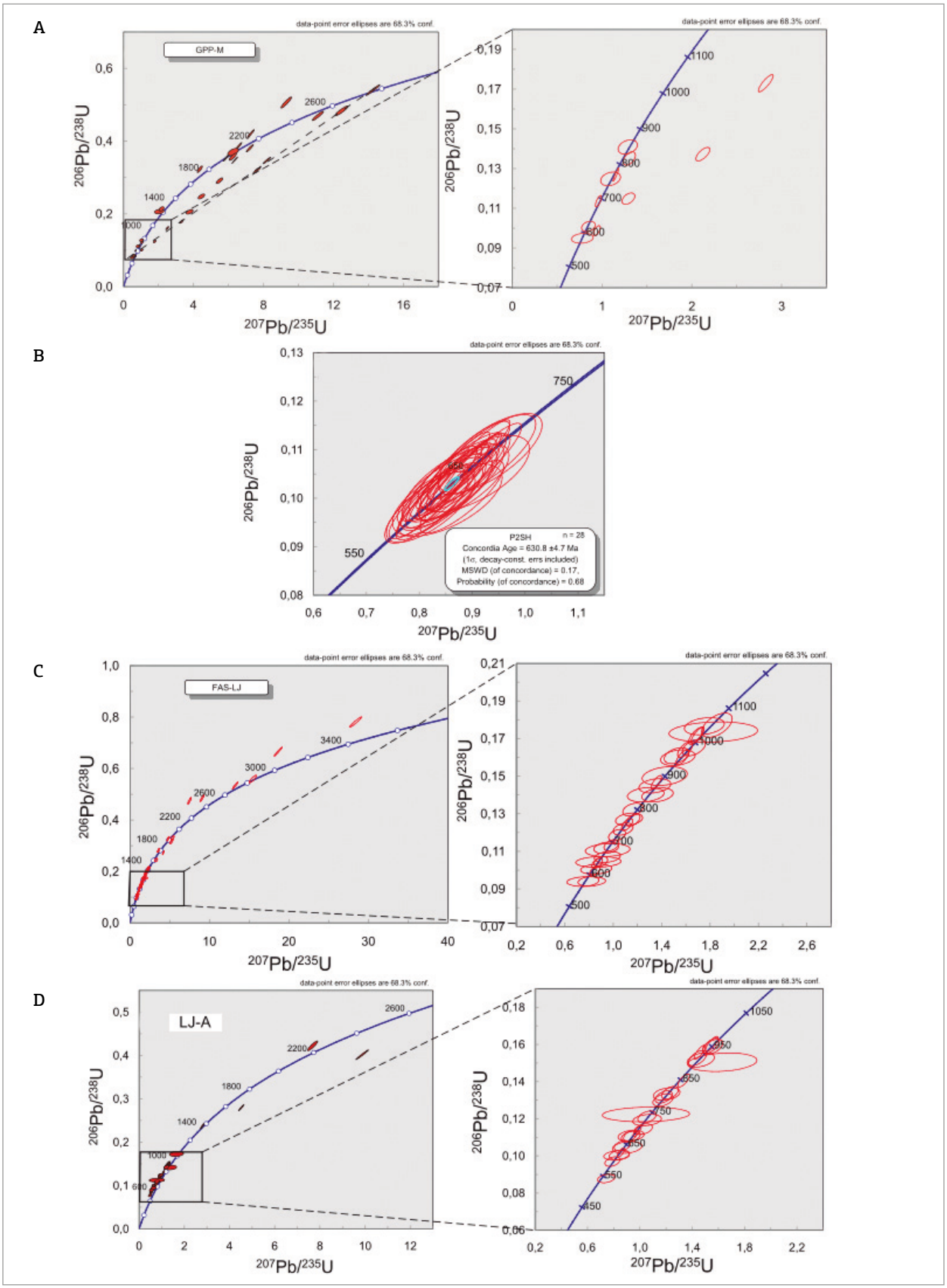

Figure 6. Concordia diagrams of the U-Pb data from detrital zircon grains: (A) sample GPP-M (Sete Lagoas Formation); (B) sample P2SH (Serra de Santa Helena Formation); (C) sample FAS-LJ (Lagoa do Jacaré Formation); (D) sample LJ-A (Lagoa do Jacaré Formation).

feeding in response to the marine transgression that flooded the craton.

Provenance studies in the Carrancas Formation conglomerates reveal a wide range of clast assemblage varying from monomitic (Guacaneme *et al.* 2017) to oligomitic (Kuchenbecker 2011, Vieira *et al.* 2007) and polimitic (Caxito *et al.* 2012, Uhlein *et al.* 2016). The occurrence of the unit described by Guacaneme *et al.* (2017) in Inhaúma city area is emblematic, as the conglomerate is clearly deposited in a basement valley and only has clasts of the leucogranite, which can be observed in the valley walls (Fig. 9). The U-Pb data of detrital zircons of the Carrancas conglomerate also point to a dominant Archean source (Kuchenbecker 2011, Guacaneme 2015) with only a few zircon grains older or younger than this main source, which is consistent with the age of the basement in the southern sector of the basin (Teixeira *et al.* 2000). These studies agree with our Sm-Nd T_{DM} ages and negative $\varepsilon_{Nd(550\ Ma)}$ values (Tab. 1; Fig. 4), that suggest Archean basement sources with very long crustal residence time. Similar results were also obtained for the Carrancas Formation by Uhlein *et al.* (2016). This data set is compatible with a very close igneous

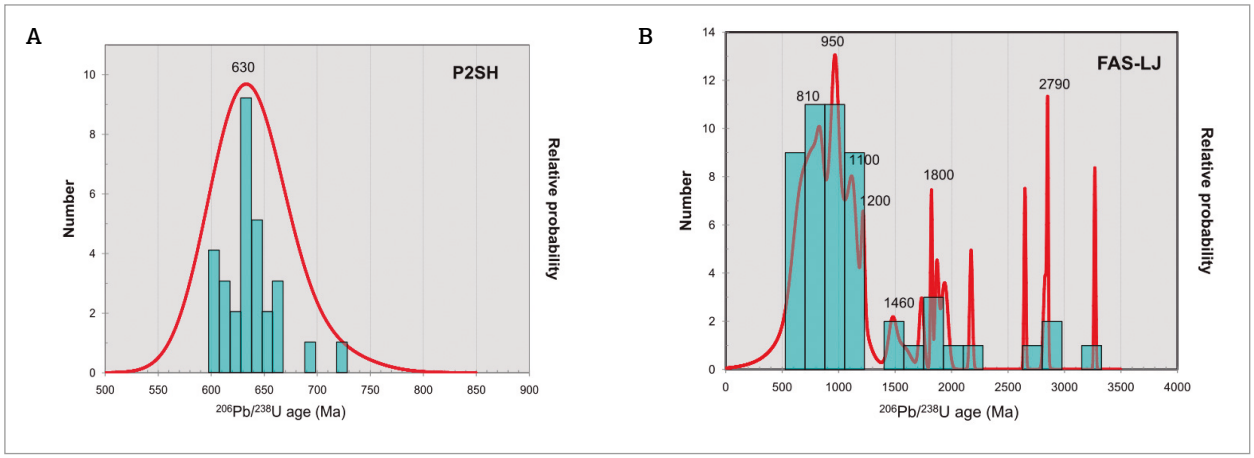

Figure 7. U-Pb age distribution histograms for samples: (A) P2SH (Serra de Santa Helena Formation); (B) FAS-LJ (Lagoa do Jacaré Formation).

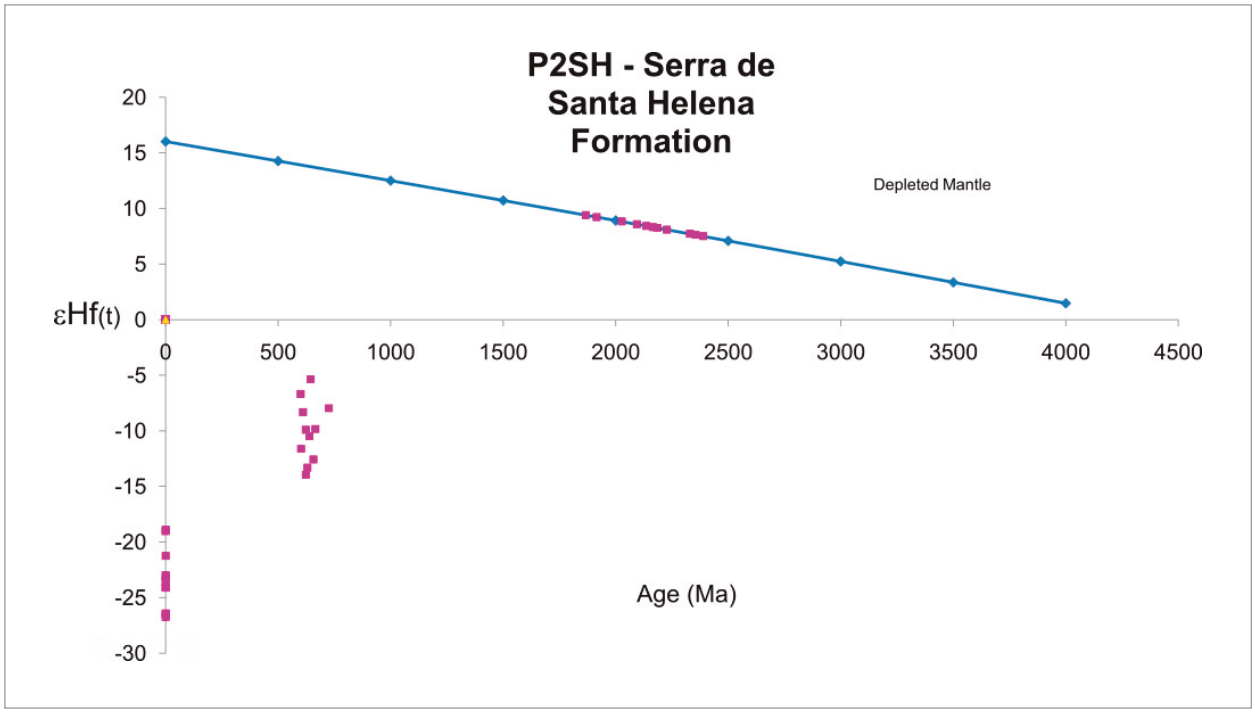

Figure 8. εHf evolution diagram for the detrital zircon grains of sample P2SH (Serra de Santa Helena Formation).

source for the conglomerates and a small area of sediment sources, derived mainly from the basement valley walls in which they were deposited (Vieira *et al.* 2007, Guacaneme *et al.* 2017). As transgression progressed and flooded the craton, the area of sedimentation extrapolated the limits of these valleys, resulting in deposition of the fine sediments in a larger area and apparently increasing the number of source areas that were initially restricted to the valley walls (Fig. 9). These new sources were potentially younger than the Archean ones. This occurrence is recorded in the transition to the finer facies in the Carrancas Formation, and in the Moema Laminites and their younger Sm-Nd T_{DM} ages and less negative $\varepsilon_{Nd(550\ Ma)}$ values. The diversification of sources may be also recorded in the U-Pb ages observed in detrital zircon grains of the Carrancas Formation siltites (sample P12, Tab. 7). The most concordant ages (discordance ≤ 3%) are from the Staterian (~1900 Ma) and Ediacaran (600 Ma) periods, with one grain dated at 485 Ma. This young age could bring about several problems concerning the basin evolution, age of glaciation and even the appearance of the *Cloudina* sp. fossil in the Bambuí Group. But we note that these data are not statistically significant for a provenance study and are not reliable for interpretation. We show the data here so other researchers may have the opportunity to better evaluate them in the future.

On the other hand, the transition from the finer facies of the Carrancas Formation and the Moema Laminites to the Bambuí Group is not marked by any significant changes in the Sm-Nd T_{DM} ages and $\varepsilon_{Nd(550\ Ma)}$ values. Sm-Nd isotopic data from bulk rock sediments are not adequate to constrain the timing of the deposition, as the T_{DM} ages represent a mixture of sources and rocks with younger detrital zircons that may yield older T_{DM} ages (Paula-Santos *et al.* 2015). Nevertheless, the striking similarity of data from those units suggests that sources with similar origin were active during most of the deposition of the São Francisco Basin. The database of U-Pb dating in detrital zircons from the Bambuí Group also show a wide range of sources spanning from the Archean to the Early Cambrian (Rodrigues 2008, Pimentel *et al.* 2011, Kuchenbecker 2014, Paula-Santos *et al.* 2015, this work), which is consistent with our interpretation for the Sm-Nd data. This adds another argument for the similarity of the sources through the deposition of the lower units and the Bambuí Group. However, tracking whether these sources are located in the Brasília or in the Araçuaí Belt is not just a single task.

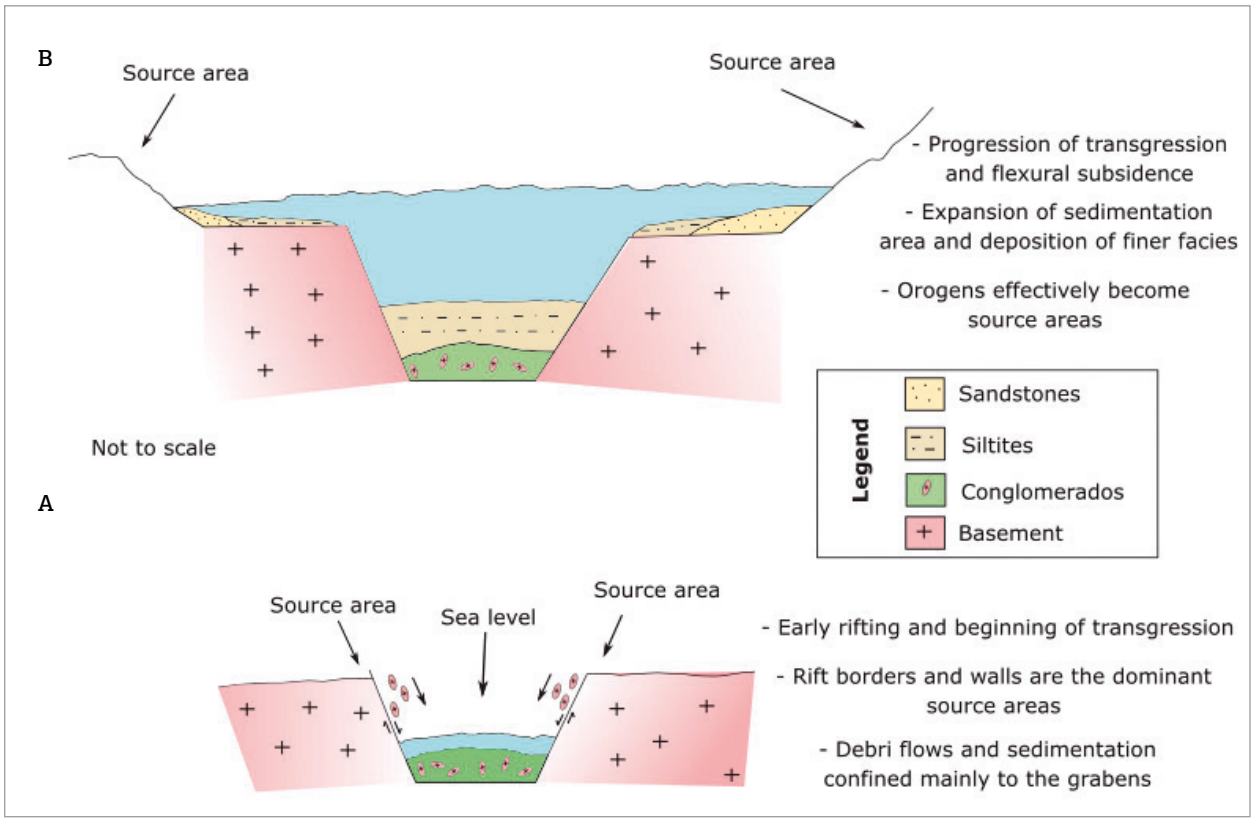

Figure 9. A sketch showing the change in the source areas during the deposition of the Carrancas Formation. The early rift borders and walls are dominant sources during the beginning of transgression (A), whereas these areas largely expand with the progression of transgression and deposition of the finer facies (B)

The T_{DM} ages between 1.3 and 2.1 Ga and $\varepsilon_{Nd(550\ Ma)}$ values between -9.53 to -4.09 are compatible with the Sm-Nd signatures of igneous rocks from both the western Brasília (Pimentel *et al*. 1999, Pimentel 2016) and the eastern Araçuaí belt (Pedrosa-Soares *et al*. 2011). Our exclusively negative $\varepsilon_{Hf(t)}$ values do not help solve the question as they mainly point to sources with a long crustal residence time.

The U-Pb ages of the detrital zircon grains from sample P2SH (Serra de Santa Helena Formation) are also dubious. The data indicate a single dominant source of ca. 630 Ma (Figs. 6B and 7A). Igneous rocks with this U-Pb age range are also found in both orogens. Collisional magmatism from the Late Cryogenian / Early Ediacaran periods is reported in the Brasília Belt (Valeriano *et al*. 2008, Seer & Moraes 2013) and in the Rio Doce magmatic arc of the Araçuaí Belt (Pedrosa-Soares *et al*. 2007, Tedeschi 2013).

The Archean and Paleoproterozoic zircon grains from the studied samples are derived from sources of the São Francisco Basin basement (Teixeira *et al*. 2000). Sources in the 1400–1050 Ma interval occur in the Mesoproterozoic basement of the Brasília Belt (Pimentel *et al*. 1999, Pimentel 2016) and in the Araçuaí Belt. Zircon grains from crystal-tuff (Guadagnin *et al*. 2015) were dated at ca. 1.4 Ga and volcanoclastic rocks (Chaves *et al*. 2013) with ages close to 1.2 Ga occur in the Espinhaço Supergroup. Detrital zircon populations within this interval age were also obtained in the Macaúbas Group (Babinski *et al*. 2012) and in the Espinhaço Supergroup (Valladares *et al*. 2004, Valeriano *et al*. 2004, Chemale Jr. *et al*. 2012), both of which are located in the eastern belt, and in the Paranoá, Canastra, Araxá and Ibiá groups of the western belt (Pimentel *et al*. 2011, Pimentel 2016). These units could have been reworked and they possibly provided sediments to the São Francisco Basin.

The Tonian sources dated around 950 Ma in sample FAS-LJ were also observed in samples GPP-M and LJ-A and may come from the Mayubian and Zanadian Groups, West-Congo orogen (Tack *et al*. 2001). However, sources with these ages are also found in the Goiás Magmatic arc of the Brasília Belt (Pimentel & Fuck 1992).

Sources dated around 800 Ma could be represented by the metagranitoids of the Arenópolis arc of the Brasília Belt dated at ca. 790 Ma (Laux *et al*. 2005). Sources with similar ages are also described in the Rio Negro Complex, located from the Ribeira Belt to the south of the São Francisco craton (Tupinambá *et al*. 2000, Heilbron & Machado 2003).

Finally, zircon grains younger than 540 Ma can also have their sources in the G4 and G5 supersuites of the Araçuaí Belt (Pedrosa-Soares *et al*. 2011) or in the Novo Brasil wedge of the Brasília Belt (Araújo 2014). In conclusion, our data do not allow for the orogen the sediments came from to be determined.

Studies using seismic sections across the São Francisco Basin suggest that the Brasília Belt is the main source of sediments for the Bambuí Group, with the Araçuaí belt working mainly as a deformer of the unit (Zalán & Romeiro-Silva 2007). Nonetheless, some authors suggest a contribution of sediments from the Araçuaí Belt to the upper Três Marias Formation (Chiavegatto 1992, Martins-Neto & Alkmim 2001). The Late Ediacaran and Cambrian ages also suggest a contribution from both orogens with important implications for the São Francisco Basin evolution. They imply a problematic time gap between the start of the São Francisco Basin subsidence and its filling. The continental collisions at the western margin of the São Francisco craton at ca. 630 Ma (Valeriano *et al*. 2004, Pimentel 2016) would mark the beginning of the accommodation space in the basin. Unless an unconformity between older units and the Late Ediacaran succession is assumed, the basin would have starved for ca. 80 (or 200) m.y., which is not plausible. Some authors point to a possible unconformity between the basal cap carbonates of the Bambuí Group and the rest of the unit (Martins & Lemos 2007, Zalán & Romeiro-Silva 2007, Uhlein *et al*. 2017). However, sedimentary and isotopic studies in complete borehole and field sections do not support a sedimentation gap of such magnitude at this stratigraphic level (Kuchenbecker *et al*. 2016, Perrella Jr. *et al*. 2017). Therefore, we argue that refinements between the subsidence and the filling histories of the São Francisco Basin are required.

Additionally, if the Araçuaí Belt is indeed source to the Bambuí Group, our U-Pb data and other data published so far for the basin may have implications for the eastern orogen. In a recent compilation of the U-Pb ages of detrital zircon from the Bambuí Group, Kuchenbecker (2014) observed that the Neoproterozoic sources of the unit have predominantly a Late Cryogenian to Early Ediacaran age (~630 Ma) with very few Late Ediacaran to Early Cambrian ages, which is consistent with the data obtained in this work. These younger sources are widely exposed in the Araçuaí belt and are grouped in the G3, G4 and G5 supersuites (Pedrosa-Soares *et al*. 2011). Considering the presence of the *Cloudina* sp. (Warren *et al*. 2014) and the age of the occurrence of this index fossil between 550-542 Ma (Grotzinger *et al*. 2000), it seems that G3 to G4 rocks were scarcely exposed during the deposition of the Bambuí Group, although they were already crystallized.

To summarize, the geochronological data obtained in this work point to only one major reorganization in the source feeding the basin during the evolution of the São Francisco Basin. This event occurs between the conglomeratic and

finer facies of the Carrancas Formation and of the Moema Laminites. It is interpreted as an expansion of the sedimentation and the area feeding the basin due to the initial marine transgression that flooded the São Francisco craton. In this scenario, the deposition initially confined within the valleys extrapolated these areas, depositing sediments derived from a larger area. Unfortunately, our data do not allow to distinguish sources that were located in the Brasília Belt, the Araçuaí belt or even in the Ribeira Belt. This question has yet to be answered and is crucial to solve the geological puzzle involving the evolution of the basin and its surrounding mobile belts.

Possible implications for the age of the glaciation

The age of the glacial unit at the base of the São Francisco Basin remains controversial, as several proposals from the Early Cryogenian (Sturtian age; Babinski *et al.* 2007), Late Cryogenian (Marinoan age; Caxito *et al.* 2012, Alvarenga *et al.* 2014, Uhlein *et al.* 2016) to Late Ediacaran ages (~550 Ma; Kuchenbecker *et al.* 2016) have been made.

The age of the middle portion of the Sete Lagoas Formation (CI-2 stage of Paula-Santos *et al.* 2017) is constrained by the index fossil *Cloudina* sp. between 550–542 Ma (Warren *et al.* 2014). The presence of detrital zircon grains younger than 540 Ma in the upper Sete Lagoas (Paula-Santos *et al.* 2015) and in the Serra da Saudade formations (Kuchenbecker 2014) suggest that the deposition of the Bambuí Group may have spanned through the Cambrian. Assuming any of the Cryogenian ages for the glacial deposits, the Late Ediacaran age for the base of the Bambuí Group implies that either the first 100 m of the Sete Lagoas Formation records 85 or 200 Myr of deposition or an unconformity yet to be found exists between the CI-1 and CI-2 carbonates. The first option is highly unlikely, as such durations are not compatible with a second order or a third order sequence (Vieira *et al.* 2007, Perrella Jr. *et al.* 2017) subdivision of the lower Sete Lagoas Formation (Vail *et al.* 1991). Here, we examine the second option and its implications.

Although some works have discussed a possible unconformity at the base of the Sete Lagoas Formation (Martins & Lemos 2007, Zalán & Romeiro-Silva 2007, Uhlein *et al.* 2017), stratigraphic (Kuchenbecker *et al.* 2016), sequence stratigraphic (Vieira *et al.* 2007, Perrella Jr. *et al.* 2017) and isotope chemostratigraphic data (Paula-Santos *et al.* 2017, Perrella Jr. *et al.* 2017) argue against the existence of an unconformity at the base of the Bambuí Group, and suggest a continuous deposition through the cap carbonates to the *Cloudina* bearing strata.

The C isotope data of the carbonates from the Sapé profile of Perrella Jr. *et al.* (2017) is especially important, as it shows that the recoveries of the $\delta^{13}C$ values from very negative to 0‰ are not sharp when the geological record is not condensed or incomplete. Additionally, Paula-Santos *et al.* (2017) suggested that the initial increase in $^{87}Sr/^{86}Sr$ isotope ratios from 0.7074 to 0.7082 in the cap carbonate (Babinski *et al.* 2007) is not a peak, but rather, they stabilize close to 0.7085 in the CI-2. This also suggests that there is no major hiatus or a long-lived sedimentation history between the cap carbonates and the remaining lower Sete Lagoas Formation. Furthermore, sequence stratigraphy studies point to no sequence boundary between the cap carbonates and the *Cloudina* bearing strata (Vieira *et al.* 2007, Perrella Jr. *et al.* 2017) as previously suggested (Martins & Lemos 2007). Both successions are grouped into one single second or third order sequence. A significant unconformity was also not observed in a complete borehole section at the south of the São Francisco Basin (Kuchenbecker *et al.* 2016).

In summary, several arguments suggest that no major unconformity or long-lived sedimentation period occurred between the cap carbonates and the rest of the Bambuí Group. We add to these arguments our Sm-Nd data that also point to no major reorganization of the basin sources during this stage. Assuming that no hiatus in the deposition exists, the glaciation may be Late Ediacaran in age, following what was recently proposed by Kuchenbecker *et al.* (2016). As no extremely negative $\delta^{13}C$ values similar to the Shuram-Wonoka anomaly (Halverson *et al.* 2005, Le Guerroué *et al.* 2006, Halverson & Hurtgen 2007) are reported for the Bambuí Group, we argue that the glaciation may be post-Gaskiers in age (≤ 582 Ma). Glaciations of this period are recorded worldwide (e.g., Frimmel *et al.* 2006, Hebert *et al.* 2010, Germs & Gaucher 2012, Ivanov *et al.* 2013, Etemad-Saeed *et al.* 2016), so the Bambuí would not be a sole case.

Although we find the possibility of an unconformity difficult to assume, it is fair to analyse the Marinoan and Sturtian propositions. The strongest argument for a Marinoan age proposition is the presence of a thin, patchy, pink cap carbonate (Caxito *et al.* 2012, Alvarenga *et al.* 2014). Such dolostone strata are described worldwide as being atop Late Cryogenian diamictites and are considered the base of the Ediacaran period (Shields 2005). Indeed, this is a robust argument, as such rocks are described in many works (e.g., Martins & Lemos 2007, Caxito *et al.* 2012). However, it is important to note that such cap dolostones are not spread through the whole basin. In many locations, the cap carbonates are pure limestones (Vieira *et al.* 2007, Kuchenbecker *et al.* 2016, Paula-Santos *et al.* 2017) and, although they display other "Marinoan" features (e.g. aragonite pseudomorphs), it is

expected that such global strata would be found all over the São Francisco Basin.

Other three pieces of evidence argue in favour of a Marinoan age for the glaciation. First, in the $^{87}Sr/^{86}Sr$ ratios, around 0.7075 usually reported for the Sete Lagoas Formation (Alvarenga *et al.* 2007, 2014, Misi *et al.* 2007, Paula-Santos *et al.* 2015), which were interpreted to reflect global seawater values after the Marinoan period (Caxito *et al.* 2012, Alvarenga *et al.* 2014). This interpretation was ruled out by Paula-Santos *et al.* (2017), who suggested that these Sr isotopic ratios are the result of restriction and local factors, and therefore cannot be used for global correlations. Furthermore, those ratios are found in carbonates atop the *Cloudina* bearing strata. The second piece of evidence is the negative C isotope excursion observed in the cap carbonates (Alvarenga *et al.* 2007, Kuchenbecker *et al.* 2016), which is more typical of post-Marinoan cap carbonates (Hoffman & Schrag 2002, Halverson *et al.* 2005). We note that such an excursion was recently reported for cap carbonates overlying glacial deposits with a maximum depositional age of 560 Ma in Iran (Etemad-Saeed *et al.* 2016) and is also expected for many glacial periods through the Ediacaran (Hebert *et al.* 2010). The third piece of evidence is the very positive $\delta^{13}C$ values of carbonate rocks of the Carrancas Formation that were correlated to the pre-Marinoan "Keele Peak" (Uhlein *et al.* 2016). Again, these $\delta^{13}C$ values are also observed in Ediacaran carbonate successions and precede negative C isotope excursions up to the Ediacaran-Cambrian Boundary (Pelechaty *et al.* 1996, Saylor *et al.* 1998, Hebert *et al.* 2010). So, we note that whereas most of the isotopic evidence could serve as arguments for a Marinoan glaciation, it could also be used to sustain a proposal for the Late Ediacaran.

The Sturtian age proposition for the basin glaciation relies on the whole rock Pb-Pb isochron age of 740 ± 22 Ma, obtained in the cap carbonates at the Sambra Quarry (Babinski *et al.* 2007). This is the only absolute age available for the cap carbonates. The isochron is of good quality, refuting any possibility of analytical problems. Nevertheless, this age would imply a ca. 200 m.y. gap between CI-1 and CI-2, which seems inconsistent with other stratigraphic and isotopic evidence. Alternatively, we may be dealing with two cap carbonate levels in the basin, which would correspond to two different diamictites of distinct ages. However, this hypothesis has no evidence to support it, and should be further investigated.

In conclusion, although neither a Sturtian nor a Marinoan age for the São Francisco Basin glaciation can be discarded, the evidence herein discussed suggests that an unconformity at the base of the Sete Lagoas Formation is unlikely to exist. Therefore, the presence of the *Cloudina* index fossil and of detrital zircon grains younger than 540 Ma in the Bambuí Group suggest that such glaciation is most likely Late Ediacaran in age.

CONCLUSIONS

The new geochronological data obtained in this work provided further insights in the evolution of the São Francisco Basin. Based on the Sm-Nd, U-Pb and Hf isotope data of siliciclastic rocks we state the following:

- the Sm-Nd isotope data from the lower glacial units and from the Bambuí Group show only one major reorganization of the sedimentary sources through the evolution of the São Francisco Basin. This is observed in the transition from the conglomerates to the finer sediments in the Carrancas Formation and the Moema Laminites, in which the T_{DM} ages abruptly fall from 2.7–3.3 Ga to ages younger than 2.1 Ga and the $\varepsilon_{Nd(550\ Ma)}$ values increase from lower than -17 to higher than -10. These isotope data reflect the change in the sedimentation initially confined to basement valleys, with sediments coming exclusively from the Archean rocks of the valley walls, to a wider basin area with deposition of the finer sediments and a larger source area. During the latter stage, the São Francisco Basin received sediments not only from the homonymous craton basement, but also from rocks located in the marginal mobile belts;
- T_{DM} ages between 1.3 and 2.1 Ga and $\varepsilon_{Nd(550\ Ma)}$ values between -9.53 to -4.09 are constantly observed from the siltites and claystones of the Carrancas Formation and the Moema Laminites up to the Lagoa do Jacaré Formation of the Bambuí Group, without significant variations. This adds another argument to support the lack of an unconformity between the lower glacial units and the Bambuí Group. Based on the presence of the index fossil *Cloudina* sp. in the lower Sete Lagoas Formation, the glaciation recorded in the São Francisco Basin is most likely Late Ediacaran in age. Nevertheless, older age propositions should not be entirely ruled out until further and more robust evidence is found;
- our geochronological data do not allow tracking whether the Ediacaran sources are located in the Brasília or in the Araçuaí Belt. Nonetheless, with ages younger than 540 Ma occurring in the Bambuí Group, better refinements in the timing between the flexural subsidence and the filling of the basin are required.

ACKNOWLEDGEMENTS

We would like to thank Professor Matheus Kuchenbecker for field work support. We would also like to thank Professor Fabrício Caxito, the anonymous reviewer, and the associate Editor Carlos Alvarenga for the comments that greatly improved the paper. The CPGeo-USP, INCT-CNPq

and the São Paulo Research Foundation (FAPESP) grant #2016/06114-6 provided support and funding for the analyses. This research is also related to the Research Group NAP-GEO-SEDex (Geodynamic of Sedimentary Basins and implications for exploration potential). Gustavo Paula-Santos received a PRH-Petrobras scholarship and currently has a FAPESP post-doc grant #2017/00399-1. Marly Babinski has a CNPq Research Fellowship.

REFERENCES

Alkmim F.F. & Martins-Neto M.A. 2012. Proterozoic first-order sedimentary sequences of the São Francisco craton, eastern Brazil. *Marine and Petroleum Geology*, **33**(1):127-139. DOI: 10.1016/j.marpetgeo.2011.08.011

Alkmim F.F., Marshak S., Pedrosa-Soares A.C., Peres G.G., Cruz S.C., Whittington A. 2006. Kinematic evolution of the Araçuaí-West Congo orogen in Brazil and Africa: Nutcracker tectonics during the Neoproterozoic assembly of Gondwana. *Precambrian Research*, **149**:43-63. DOI: 10.1016/j.precamres.2006.06.007

Alvarenga C.J.S., Della Giustina M.E.S., Silva N.G.C., Santos R.V.S., Gioia S.M.C.L., Guimarães E.M., Dardenne M.A., Sial A.N., Ferreira V.P. 2007. Variações dos isótopos de C e Sr em carbonatos pré e pós-glaciação Jequitaí (Esturtiano) na região de Bezerra-Formosa, Goiás. *Revista Brasileira de Geociências*, **37**(4):147-155.

Alvarenga C.J.S., Santos R.V., Vieira L.C., Lima B.A.F., Mancini L.H. 2014. Meso-Neoproterozoic isotope stratigraphy on carbonates platforms in the Brasilia Belt of Brazil. *Precambrian Research*, **251**:164-180. https://doi.org/10.1016/j.precamres.2014.06.011

Araújo J.G.M. 2014. *Eventos ígneos e metamórficos neoproterozoicos / eo-paleozoicos no Arco Magmático de Arenópolis, Goiás*. PhD Thesis, Instituto de Geociências da Universidade de Brasília, Brasília, 73 p.

Babinski M., Pedrosa-Soares A.C., Trindade R.I.F., Martins M., Noce C.M., Liu D. 2012. Neoproterozoic glacial deposits from the Araçuaí orogen, Brazil: Age, provenance and correlations with the São Francisco craton and West Congo belt. *Gondwana Research*, **21**:451-465. DOI: 10.1016/j.gr.2011.04.008

Babinski M., Vieira L.C., Trindade R.I.F. 2007. Direct dating of Sete Lagoas cap carbonate (Bambuí Group, Brazil) and implications for the Neoproterozoic glacial events. *Terra Nova*, **19**:401-406. DOI: 10.1111/j.1365-3121.2007.00764.x

Black L.P., Kamo S.L., Allen C.M., Aleinikoff J.N., Davis D.W., Korsch R.J., Foudoulis C. 2003. TEMORA 1: a new zircon standard for Phanerozoic U-Pb geochronology. *Chemical Geology*, **200**:155-170. https://doi.org/10.1016/S0009-2541(03)00165-7

Blichert-Toft J. & Albarède F. 1997. The Lu-Hf isotope geochemistry of chondrites and the evolution of the mantle crust system. *Earth and Planetary Science Letters*, **148**:243-258. https://doi.org/10.1016/S0012-821X(97)00040-X

Caxito F.A., Halverson G.P., Uhlein A., Stevenson R., Dias T.G., Uhlein G.J. 2012. Marinoan glaciation in east Central Brazil. *Precambrian Research*, **200-203**:38-58. https://doi.org/10.1016/j.precamres.2012.01.005

Chaves M.L.S.C., da Silva M.C.S., Scholz R., Babinski M. 2013. Grenvillian age magmatism in the Southern Espinhaço Range (Minas Gerais): evidence from U-Pb zircon ages. *Brazilian Journal of Geology*, **43**(3):477-486.

Chaves M.L.S.C., Guimarães J.T., Andrade K.W. 2010. Litofácies glaciomarinhas na Formação Jequitaí: possíveis implicações na redistribuição de diamantes a oeste da Serra do Espinhaço (MG). *Revista Brasileira de Geociências*, **40**(4):516-526.

Chemale Jr. F., Dussin I.A., Alkmim F.F., Martins M.S., Queiroga G., Armstrong R., Santos M.N. 2012. Unravelling a Proterozoic basin history through detrital zircon geochronology: The case of the Espinhaço Supergroup, Minas Gerais, Brazil. *Gondwana Research*, **22**(1):200-206. https://doi.org/10.1016/j.gr.2011.08.016

Chiavegatto J.R.S. 1992. *Análise estratigráfica das sequências tempestíticas da Formação Três Marias (Proterozoico Superior), na porção meridional da Bacia do São Francisco*. Master Dissertation, Universidade Federal de Ouro Preto, Ouro Preto, 216 p.

Coelho M.B., Trouw R.A.J, Ganade C.E., Vinagre R., Mendes J.C., Sato K. 2017. Constraining timing and P-T conditions of continental collision and late overprinting in the Southern Brasília Orogen (SE-Brazil): U-Pb zircon ages and geothermobarometry of the Andrelândia Nappe System. *Precambrian Research*, **292**:194-215. DOI: 10.1016/j.precamres.2017.02.001

Cukrov N., Alvarenga C.J.S., Uhlein A. 2005. Litofácies da glaciação neoproterozoica nas porções sul do Cráton do São Francisco: exemplos de Jequitaí (MG) e Cristalina (GO). *Revista Brasileira de Geociências*, **35**:69-76.

Dardenne M.A. 1978. Síntese sobre a estratigrafia do Grupo Bambuí no Brasil Central. *In*: SBG, Congresso Brasileiro de Geologia, 30, Recife, Brazil. *Anais*, v. 2, p. 597-610.

Dardenne M.A. 2000. The Brasília fold belt. *In*: Cordani U.G., Milani E.J., Thomaz-Filho A., Campos D.A. (eds.). Tectonic Evolution of South America, *31st International Geological Congress*, Rio de Janeiro, p. 231-263.

DePaolo D. 1981. Neodymium isotopes in the Colorado Front Range and crust-mantle evolution in the Proterozoic. *Nature*, **291**:193-196. DOI: **10.1038/291193a0**

Etemad-Saeed N., Hosseini-Barzi M., Adabi M.H., Miller N.R., Sadeghi A., Houshmandzadeh A., Stockli D.F. 2016. Evidence for ca. 560 Ma Ediacaran glaciations in the Kahar Formation, central Alborz Mountains, northern Iran. *Gondwana Research*, **31**:164-183. https://doi.org/10.1016/j.gr.2015.01.005

Frimmel H.E., Tack L., Basei M.S., Nutman A.P., Boven A. 2006. Provenance and chemostratigraphy of the Neoproterozoic West Congolian Group in the Democratic Republic of Congo. *Journal of African Earth Sciences*, **46**:221-239. https://doi.org/10.1016/j.jafrearsci.2006.04.010

Germs G.J.B. & Gaucher C. 2012. Nature and extent of a Late Ediacaran (ca. 547 Ma) glaciogenic erosion surface in southern Africa. *South African Journal of Geology*, **115**(1):91-102. https://doi.org/10.2113/gssajg.115.91

Griffin W.L., Wang X., Jackson S.E., Pearson N.J., O'Reilly S.Y., Xu X., Zhou X. 2002. Zircon chemistry and magma mixing, SE China: In-situ analysis of Hf isotopes, Tonglu and Pingtan igneous complexes. *Lithos*, **61**(3-4):237-269. https://doi.org/10.1016/S0024-4937(02)00082-8

Grotzinger J.P., Watters W.A., Knoll A.H. 2000. Calcified metazoans in thrombolite-stromatolite reefs of the terminal Proterozoic Nama Group, Namibia. *Paleobiology*, **26**(3):334-359. https://doi.org/10.1666/0094-8373(2000)026%3C0334:CMITSR%3E2.0.CO;2

Guacaneme C. 2015. *Geoquímica isotópica e elementar dos carbonatos da Formação Sete Lagoas, Grupo Bambuí, no sul da bacia do São Francisco*. Master Dissertation, Instituto de Geociências da Universidade de São Paulo, São Paulo, 131 p.

Guacaneme C., Babinski M., Paula-Santos G.M., Pedrosa-Soares A.C. 2017. C, O and Sr isotopic variations in Neoproterozoic-Cambrian carbonate rocks from the Sete Lagoas Formation (Bambuí Group), in the southern São Francisco basin, Brazil. *Brazilian Journal of Geology*, **47**(3):521-543. DOI: 10.1590/2317-4889201720160126

Guadagnin F., Chemale Jr F., Magalhães A.J.C., Santana A., Dussin I., Takehara L. 2015. Age constraints on crystal-tuff from the Espinhaço Supergroup – Insight into the Paleoproterozoic to Mesoproterozoic intracratonic basin cycles of the Congo-São Francisco Craton. *Gondwana Research*, **27**(1):363-376. https://doi.org/10.1016/j.gr.2013.10.009

Halverson G.P. & Hurtgen M.T. 2007. Ediacaran growth of the marine sulfate reservoir. *Earth and Planetary Science Letters*, **263**:32-44. https://doi.org/10.1016/j.epsl.2007.08.022

Halverson G.P., Hoffman P.F., Schrag D.P., Maloof A.C., Rice A.H. 2005. Toward a Neoproterozoic composite carbon-isotope record. *GSA Bulletin*, **117**:1181-1207. https://doi.org/10.1130/B25630.1

Hamilton P.J., O'Nions R.K, Bridgwater D., Nutman A. 1983. Sm-Nd studies of Archean metassediments and metavolcanics from West Greenland and their implications for the Earth's early history. *Earth and Planetary Science Letters*, **62**(2):263-272. https://doi.org/10.1016/0012-821X(83)90089-4

Hebert C.L., Kaufman A.J., Penniston-Dorland S.C., Martin A.J. 2010. Radiometric and stratigraphic constraints on terminal Ediacaran (post-Gaskiers) glaciations and metazoan evolution. *Precambrian Research*, **182**:402-412. DOI: 10.1016/j.precamres.2010.07.008

Heilbron M. & Machado N. 2003 Timing of terrane accretion in the Neoproterozoic-Eopaleozoic Ribeira orogen (SE Brazil). *Precambrian Research*, **125**:87-112. DOI: 10.1016/S0301-9268(03)00082-2

Heilbron M., Valeriano C.M., Tassinari C.C.G., Almeida J., Tupinambá M., Siga Jr. O., Trouw R. 2008. Correlation of Neoproterozoic terranes between the Ribeira Belt, SE Brazil, and its African counterpart: comparative tectonic evolution and open questions. *Geological Society Special Publications*, **294**(1):211-237. DOI: 10.1144/SP294.12

Hoffman P.F. & Schrag D.P. 2002. The Snowball Earth hypothesis: testing the limits of global change. *Terra Nova*, **14**:129-155. DOI: 10.1046/j.1365-3121.2002.00408.x

Hoffman P.F., Kaufman A.J., Halverson G.P., Schrag D.P. 1998. A Neoproterozoic Snowball Earth. *Science*, **281**:1342-1346. DOI: 10.1126/science.281.5381.1342

Iglesias M. & Uhlein A. 2009. Estratigrafia do Grupo Bambuí e coberturas fanerozoicas no vale do rio São Francisco, norte de Minas Gerais. *Revista Brasileira de Geociências*, **39**(2):256-266.

Ivanov A.V., Mazukabzov A.M., Stanevich A.M., Palesskiy S.V., Kosmenko O.A. 2013. Testing the snowball Earth hypothesis for the Ediacaran. *Geology*, **41**(7):787-790. https://doi.org/10.1130/G34345.1

Karfunkel J. & Hoppe A. 1988. Late Precambrian glaciation in central-eastern Brazil: Synthesis and model. *Palaeogeography, Palaeoclimatology, Palaeoecology*, **65**:1-21. https://doi.org/10.1016/0031-0182(88)90108-3

Kuchenbecker M. 2011. *Quimioestratigrafia e proveniência sedimentar da porção basal do Grupo Bambuí em Arcos (MG)*. Master Dissertation, Instituto de Geociências da Universidade Federal de Minas Gerais, Belo Horizonte, 91 p.

Kuchenbecker M. 2014. *Relações entre as coberturas do Cráton do São Francisco e bacias situadas em orógenos marginais: o registro de datações U-Pb de grãos detríticos de zircão e suas implicações geotectônicas*. PhD Thesis, Instituto de Geociências da Universidade Federal de Minas Gerais, Belo Horizonte, 163 p.

Kuchenbecker M., Babinski M., Pedrosa-Soares A.C., Lopes-Silva L., Pimenta F. 2016. Chemostratigraphy of the lower Bambuí Group, southwestern São Francisco Craton, Brazil: insights on Gondwana paleoenvironments. *Brazilian Journal of Geology*, **46**(1):145-162. http://dx.doi.org/10.1590/2317-488920160030285

Laux J.H., Pimentel M.M., Dantas E.L., Armstrong R., Junges S.L. 2005. Two Neoproterozoic crustal accretion events in the Brasília belt, central Brazil. *Journal of South American Earth Sciences*, **18**:183-198. https://doi.org/10.1016/j.jsames.2004.09.003

Le Guerroué E., Allen P., Cozzi A., Etienne J.L., Fanning M. 2006. 50 Myr recovery from the largest negative $\delta^{13}C$ excursion in the Ediacaran ocean. *Terra Nova*, **18**(2):147-153. DOI: 10.1111/j.1365-3121.2006.00674.x

Ludwig K.R. 2012. User's manual for Isoplot 3.75. A geochronological toolkit for Microsoft Excel. *Special Publication*, Berkeley Geochronological Center, Berkeley, USA, 5:1-75.

Martins M. & Lemos V.B. 2007. Análise estratigráfica das sequências neoproterozoicas da Bacia do São Francisco. *Revista Brasileira de Geociências*, **37**(4):156-167.

Martins-Neto M.A. & Alkmim F.F. 2001. Estratigrafia e evolução tectônica das bacias neoproterozoicas do paleocontinente São Francisco e suas margens: Registro da quebra de Rodínia e colagem de Gondwana. *In*: Pinto C.P. & Martins-Neto M.A. (eds.). *Bacia do São Francisco: Geologia e Recursos Naturais*. SBG / Núcleo MG, 31-54.

Martins-Neto M.A. & Hercos C.M. 2002. Sedimentation and tectonic setting of Early Neoproterozoic glacial deposits in southeastern Brazil. *In*: Altermann W. & Corcoran P.L. (eds.). Precambrian Sedimentary Environments: A Modern Approach to Ancient Depositional Systems. International Association of Sedimentologists. *Special Publications*, 33:383-403.

Martins-Neto M.A., Pedrosa-Soares A.C., Lima S.A.A. 2001. Tectono-sedimentary evolution of sedimentary basins from Late Paleoproterozoic to Late Neoproterozoic in the São Francisco craton and Araçuaí fold belt, eastern Brazil. *Sedimentary Geology*, **141-142**:343-370. https://doi.org/10.1016/S0037-0738(01)00082-3

Misi A., Kaufman A.J., Veizer J., Powis K., Azmy K., Boggiani P.C., Gaucher C., Teixeira J.B.G., Sanches A.L., Iyer S.S.S. 2007. Chemostratigraphic correlation of Neoproterozoic successions in South America. *Chemical Geology*, **237**:143-167. https://doi.org/10.1016/j.chemgeo.2006.06.019

Paula-Santos G.M., Babinski M., Kuchenbecker M., Caetano-Filho S., Trindade R.I., Pedrosa-Soares A.C. 2015. New evidence for an Ediacaran age for the Bambuí Group in southern São Francisco Craton (eastern Brazil) from zircon U-Pb data and isotope chemostratigraphy. *Gondwana Research*, **28**(2):702-720. https://doi.org/10.1016/j.gr.2014.07.012

Paula-Santos G.M., Caetano-Filho S., Babinski M., Trindade R.I., Guacaneme C. 2017. Tracking connection and restriction of West Gondwana São Francisco Basin through isotope chemostratigraphy. *Gondwana Research*, **42**:280-305. https://doi.org/10.1016/j.gr.2016.10.012

Pedrosa-Soares A.C., Campos C.P., Noce C., Silva L.C., Novo T., Roncato J., Medeiros S., Castañeda C., Queiroga G., Dantas E., Dussin I., Alkmim F.F. 2011. Late Neoproterozoic-Cambrian granitic magmatism in the Araçuaí orogen (Brazil), the Eastern Brazilian Pegmatite Province and related mineral resources. *Geological Society of London Special Publications*, **350**:25-51.

Pedrosa-Soares A.C., Noce C.M., Alkmim F.F., Silva L.C., Babinski M., Cordani U., Castañeda C. 2007. Orógeno Araçuaí: síntese do conhecimento 30 anos após Almeida 1977. *Geonomos*, **15**:1-16.

Pelechaty S., Kaufman A.J., Grotzinger J.P. 1996. Evaluation of $\delta^{13}C$ isotope stratigraphy for intrabasinal correlation: data from Vendian strata of the Olenek uplift and Kharaulakh Mountains, Siberian Platform, Russia. *GSA Bulletin*, **108**:992-1003. https://doi.org/10.1130/0016-7606(1996)108<0992:EOCCFI>2.3.CO;2

Perrella Jr. P.P., Uhlein A., Uhlein G.J., Sial A.N., Pedrosa-Soares A.C., Lima O.N.B. 2017. Facies analysis, sequence stratigraphy and chemostratigraphy of the Sete Lagoas Formation (Bambuí Group), northern Minas Gerais State, Brazil: evidence of a cap carbonate deposited on the Januária basement high. *Brazilian Journal of Geology*, **47**(1):59-77. DOI: 10.1590/2317-4889201720160112

Pimentel M.M. 2016. The tectonic evolution of the Neoproterozoic Brasília Belt, central Brazil: a geochronological and isotopic approach. *Brazilian Journal of Geology*, **46**(1):67-82. http://dx.doi.org/10.1590/2317-4889201620150004

Pimentel M.M. & Fuck R.A. 1992. Neoproterozoic crustal accretion in central Brazil. *Geology*, **20**:375-379. https://doi.org/10.1130/0091-7613(1992)020<0375:NCAICB>2.3.CO;2

Pimentel M.M., Fuck R.A., Botelho N.F. 1999. Granites and the geodynamic history of the Neoproterozoic Brasília belt, Central Brazil: A review. *Lithos*, **46**(3):463-483. DOI: 10.1016/S0024-4937(98)00078-4

Pimentel M.M., Rodrigues J.B., Della Giustina M.E.S., Junges S., Matteini M., Armstrong R. 2011. The tectonic evolution of the Neoproterozoic Brasília Belt, central Brazil, based on SHRIMP and LA-ICPMS U-Pb sedimentary provenance data: a review. *Journal of South American Earth Sciences*, **31**:345-357. https://doi.org/10.1016/j.jsames.2011.02.011

Reis H.L.S. & Suss J.F. 2016. Mixed carbonate-siliciclastic sedimentation in forebulge grabens: an example from the Ediacaran Bambuí Group, São Francisco Basin, Brazil. *Sedimentary Geology*, **339**:83-103. https://doi.org/10.1016/j.sedgeo.2016.04.004

Rocha-Campos A.C. & Hasui Y. 1981. Tillites of the Macaúbas Group (Proterozoic) in central Minas Gerais and southern Bahia, Brazil. *In*: Hambrey M.J., Harland W.B. (eds.). *Earth's pre-Pleistocene Glacial Record*. Cambridge, Cambridge University Press, p. 933-939.

Rocha-Campos A.C., Brito-Neves B.B., Babinski M., Santos P.R., Oliveira S.M.B., Romano A. 2011. Moema Laminites: a newly recognized Neoproterozoic (?) glaciogenic unit, São Francisco Basin, Brazil. *Geological Society London Memoirs*, **36**:535-540.

Rocha-Campos A.C., Young G.M., Santos P.R. 1996. Re-examination of a striated pavement near Jequitaí, MG: implications for Proterozoic stratigraphy and glacial geology. *Anais da Academia Brasileira de Ciências*, **68**(4):593.

Rodrigues J.B. 2008. *Proveniência de sedimentos dos grupos Canastra, Ibiá, Vazante e Bambuí – um estudo de zircões detríticos e idades modelo Sm-Nd*. PhD Thesis, Instituto de Geociências, Universidade de Brasília, Brasília, 128 p.

Saylor B.Z., Kaufman A.J., Grotzinger J.P., Urban F. 1998. A composite reference section for terminal Proterozoic strata of the southern Namibia. *Journal of Sedimentary Research*, **68**:1223-1235. DOI: 1073-130X/98/068-1223/$03.00

Seer H.J. & Moraes L.C. 2013. Within plate, arc and collisional Neoproterozoic granitic magmatism in the Araxá Group, Southern Brasília belt, Minas Gerais, Brazil. *Brazilian Journal of Geology*, **43**(2):333-354. DOI: 10.5327/Z2317-48892013000200010

Shields G.A. 2005. Neoproterozoic cap carbonates: a critical appraisal of existing models and the plumeworld hypothesis. *Terra Nova*, **17**:299-310. DOI: 10.1111/j.1365-3121.2005.00638.x

Söderlund U., Patchett P.J., Vervoot J.D., Isachsen C.E. 2004. The ^{176}Lu decay constant determined by Lu-Hf and U-Pb isotope systematic of Precambrian mafic intrusions. *Earth and Planetary Science Letters*, **219**(3-4):311-324. https://doi.org/10.1016/S0012-821X(04)00012-3

Steiger R.H. & Jäger E. 1977. Subcommission on geochronology: convention on the use of decay constants in geo- and cosmochronology. *Earth and Planetary Science Letters*, **36**:359-362. https://doi.org/10.1016/0012-821X(77)90060-7

Tack L., Wingate M.T.D., Liegeois J.P., Fernandez-Alonso M., Deblond A. 2001. Early Neoproterozoic magmatism (1000-910 Ma) of the Zadinian and Mayumbian Groups (Bas-Congo): Onset of Rodinian rifting at the western edge of the Congo craton. *Precambrian Research*, **110**:277-306. DOI: 10.1016/S0301-9268(01)00192-9

Tedeschi M.F. 2013. *Caracterização do Arco Magmático do Orógeno Araçuaí entre Frei Inocêncio e Itambacuri, MG*. Master Dissertation, Instituto de Geociências, Universidade Federal de Minas Gerais, Belo Horizonte, 127 p.

Teixeira W., Sabaté P., Barbosa J., Noce C.M., Carneiro M.A. 2000. Archean and Paleoproterozoic tectonic evolution of the São Francisco craton, Brazil. *In*: Cordani U.G., Milani E.J., Thomaz-Filho A., Campos D.A. (eds.). *Tectonic Evolution of South America*. 31st International Geology Congress, Rio de Janeiro, 101-137.

Tupinambá M., Teixeira W., Heilbron M. 2000. Neoproterozoic Western Gondwana assembly and subduction-related plutonism: the role of the Rio Negro Complex in the Ribeira Belt, Southern Brazil. *Revista Brasileira de Geociências*, **30**:7-11.

Uhlein A., Alvarenga C.J.S., Dardenne M.A., Trompette R.R. 2011. The glaciogenic Jequitaí Formation, southeastern Brazil. *In*: Arnaud E., Halverson G.P., Shields-Zhou G. (eds.). The Geological Record of Neoproterozoic Glaciations. *Geological Society London Memoirs*, **36**:51-66.

Uhlein A., Trompette R., Alvarenga C. 1999. Neoproterozoic glacial and gravitational sedimentation on a continental rifted margin: The Jequitaí-Macaúbas sequence (Minas Gerais, Brazil). *Journal of South American Earth Sciences*, **12**:435-451. https://doi.org/10.1016/S0895-9811(99)00032-2

Uhlein G.J., de Carvalho J.F.M.G., Uhlein A., Caxito F.A., Halverson G.P., Sial A.N. 2012. Estratigrafia e sedimentologia da Formação Carrancas, Grupo Bambuí, nas regiões de Belo Horizonte e Pitangui, MG. *Geonomos*, **20**(2):79-97. http://dx.doi.org/10.18285/geonomos.v2i20.250

Uhlein G.J., Uhlein A., Halverson G.P., Stevenson R., Caxito F.A., Cox G.M., Carvalho J.F.M.G. 2016. The Carrancas Formation, Bambuí Group: A record of pre-Marinoan sedimentation on the southern São Francisco craton, Brazil. *Journal of South American Earth Sciences*, **71**:1-16. https://doi.org/10.1016/j.jsames.2016.06.009

Uhlein G.J., Uhlein A., Stevenson R., Halverson G.P., Caxito F.A., Cox G.M. 2017. Early to Late Ediacaran conglomeratic wedges from a complete foreland basin cycle in the southwest São Francisco Craton, Bambuí Group, Brazil. *Precambrian Research*, **299**:101-116. https://doi.org/10.1016/j.precamres.2017.07.020

Vail P.R., Audermard F., Bowman S.A., Eisner P.N., Perez-Cruz C. 1991. The stratigraphic signatures of tectonics, eustasy and sedimentology: an overview. *In*: Einsele G., Ricken W., Seilacher A. (eds.). *Cycles and Events in Stratigraphy*. Berlin, Springer-Verlag, p. 617-659.

Valeriano C.M., Machado N., Simonetti A., Valladares C.S., Seer H.J., Simões L.S.A. 2004. U-Pb geochronology of Southern Brasília belt (SE-Brazil): sedimentary provenance, Neoproterozoic orogeny and assembly of West Gondwana. *Precambrian Research*, **130**:27-55.

Valeriano C.M, Pimentel M.M., Heilbron M., Almeida J.C.H., Trouw R.A.J. 2008. Tectonic evolution of the Brasília Belt, Central Brazil, and early assembly of Gondwana. *In*: Pankhurst R.J., Trouw R.A.J., Brito-Neves B.B., De Wit M.J. (eds.). West Gondwana: Pre-Cenozoic correlations across the South Atlantic region. Geological Society, London, *Special Publications*, **294**:197-210.

Valladares C.S., Machado N., Heilbron M., Gauthier G. 2004. Ages of detrital zircon from siliciclastic successions South of the São Francisco Craton, Brazil: Implications for the evolution of Proterozoic basins. *Gondwana Research*, **7**(4):913-921. https://doi.org/10.1016/S1342-937X(05)71074-1

Vervoot J.D. & Blichert-Toft J. 1999. Evolution of depleted mantle: Hf isotope evidence from juvenile rocks through time. *Geochemica et Cosmochimica Acta*, **63**:533-566. https://doi.org/10.1016/S0016-7037(98)00274-9

Vieira L.C., Trindade R.I.F, Nogueira A.C.R., Ader M. 2007. Identification of a Sturtian cap carbonate in the Neoproterozoic Sete Lagoas carbonate plataform, Bambuí Group, Brazil. *Comptes Rendus Geoscience*, **339**:240-258. DOI: 10.1016/j.crte.2007.02.003

Warren L.V., Quaglio F., Riccomini C., Simões M.G., Poiré D.G., Strikis N.M., Anelli L.E., Strikis P.C. 2014. The puzzle assembled: Ediacaran guide fossil *Cloudina* reveals an old proto-Gondwana seaway. *Geology*, **42**(5):391-394.

Williams I.S. 1998. U-Th-Pb geochronology by ion microprobe. *In*: McKibben M.A., Shanks W.C., Ridley W.I. (eds.). Applications of microanalytical techniques to the understanding mineralizing processes. *Reviews in Economic Geology*, **7**:1-35.

Zalán P.V. & Romeiro-Silva P.C. 2007. Bacia do São Francisco. *Boletim de Geociências da Petrobras*, **15**(2):561-571.